A STRAND OF CARDIAC MUSCLE

Its Ultrastructure and the Electrophysiological Implications of Its Geometry

EDWARD A. JOHNSON and JOACHIM R. SOMMER

From the Departments of Physiology and Pathology, Duke University Medical Center, and the Veterans Administration Hospital, Durham, North Carolina

ABSTRACT

The structure of a small strand of rabbit heart muscle fibers (trabecula carnea), 30–80 μ in diameter, has been examined with light and electron microscopy. By establishing a correlation between the appearance of regions of close fiber contact in light and electron microscopy, the extent and distribution of regions of close apposition of fibers has been evaluated in approximately 200 μ length of a strand. The distribution of possible regions of resistive coupling between fibers has been approximated by a model system of cables. The theoretical linear electrical properties of such a system have been analyzed and the implications of the results of this analysis are discussed. Since this preparation is to be used for correlated studies of the electrical, mechanical, and cytochemical properties of cardiac muscle, a comprehensive study of the morphology of this preparation has been made. The muscle fibers in it are distinguished from those of the rabbit papillary muscle, in that they have no triads and have a kind of mitochondrion not found in papillary muscle. No evidence of a transverse tubular system was found, but junctions of cisternae of the sarcoplasmic reticulum and the sarcolemma, peripheral couplings, were present. The electrophysiological implications of the absence of transverse tubules are discussed. The cisternae of the couplings showed periodic tubular extensions toward the sarcolemma. A regularly spaced array of Z line–like material was observed, suggesting a possible mechanism for sarcomere growth.

INTRODUCTION

What is needed to answer some of the questions about the mechanical and electrical activity of cardiac muscle is a preparation of cardiac muscle equivalent to that of the isolated single skeletal muscle fiber of the frog.

Isolation of a single, intact and functioning, cardiac muscle fiber is not feasible. Cardiac muscle is composed of a population of small muscle fibers, about 10 μ in diameter and of relatively uncertain but short length, which are closely apposed in the region of the intercalated disc. Furthermore, the membranes of apposed cardiac muscle fibers frequently fuse with one another so that to separate them would disrupt their structure.

However, small trabeculae carneae of cardiac muscle fibers (30–80 μ in diameter) can be isolated, intact, from the rabbit right ventricle. Although smaller than a single skeletal muscle fiber of the frog, the strand is, unfortunately, composed of several fibers (about 10 μ in diameter) and hence, compared with a single skeletal muscle fiber, is a complex structure. Nevertheless, the

strand is sufficiently small to allow details of its structure to be viewed in the living state by high-power light microscopy. The contraction of single sarcomeres can be seen and microelectrodes can be inserted under direct vision at any desired point into single muscle fibers. The preparation thus succeeds in having some of the advantageous features of a skeletal muscle fiber, and, we think, it represents a considerable advance over the Purkinje strand of the ungulate and dog hearts or the conventional atrial or ventricular muscle preparations.

We intend to use the strand as a preparation for the study of some of the mechanical properties of cardiac muscle, particularly excitation-contraction coupling, and for the study of the electrophysiology of cardiac muscle. In addition, because of the small diameter of the strand, we also plan to use it as a model system of cardiac muscle for studies using ultrastructural cytochemical techniques.

Although cardiac muscle is composed of discrete cells closely apposed in the region of the intercalated disc, the cells behave electrically as a syncytium so that it is necessary that parts, at least, of the cell membranes in these regions of close apposition be of low electrical resistance. With a view to predicting theoretically the electrical behavior of such a syncytium, various approximations have been made as to the form that this syncytium might take. For the ventricular wall, these approximations range from a sheet or disclike structure (32) to a hexagonal array of interconnecting fibers (17), and a single cable for a bundle of Purkinje fibers (57, 14). These various hypothetical forms arise from differing assumptions as to the extent and frequency of low resistance connections between cells. The electrical behavior of each of these differing geometries is quite different, e.g. the relationship between the input resistance and the membrane resistance. For these reasons, it is clear that much more information is needed about the geometry of fibers in the strand, particularly the frequency and extent of close intercellular appositions.

Thus, to establish a foundation for the studies referred to above, it became imperative to describe the entire morphology of the strand in detail and, for reasons presently to be appreciated, to contrast it with the structure of the papillary muscle of the rabbit wherever necessary. Furthermore, by elucidating the frequency and distribution of close junctions between the fibers of the strand we will show that electrophysiological observations can be reconciled with a proposed theoretical model. This model approximates the probable pattern of low resistive couplings between the fibers in the strand.

METHODS

A. *Isolation of the Strand*

Rabbits were killed by a blow on the neck; the heart was excised within 30 sec and placed in a beaker of Krebs-Henseleit solution aerated with a gas mixture of 95% O_2 and 5% CO_2 at room temperature.

Symbols of Plates

A, Zonula adherens
AX, Axon
B, Basement membrane
C, Coupling
CM, Central membrane
CO, Collagen
Cr, Crista mitochondrialis
D, Macula adherens
E, Endocardium
F, Fibrocyte
G, Intercellular space
H, Multivesicular region (Golgi?)
I, I band
ID, Intercalated disc
K, Cisterna of sarcoplasmic reticulum
L, L line
LV, Large synaptic vesicle
M, M line
MF, Myofibril
Mi, Mitochondrion
MS, Special mitochondrion
N, Nucleus
O, Zonula occludens
P, "Pinocytotic" vesicle
Q, Schwann cell
S, Sarcolemma
SR, Sarcoplasmic reticulum
St, Striae
T, Transverse tubule
TF, Tubular fibril
V, Synaptic vesicle
Z, Z line

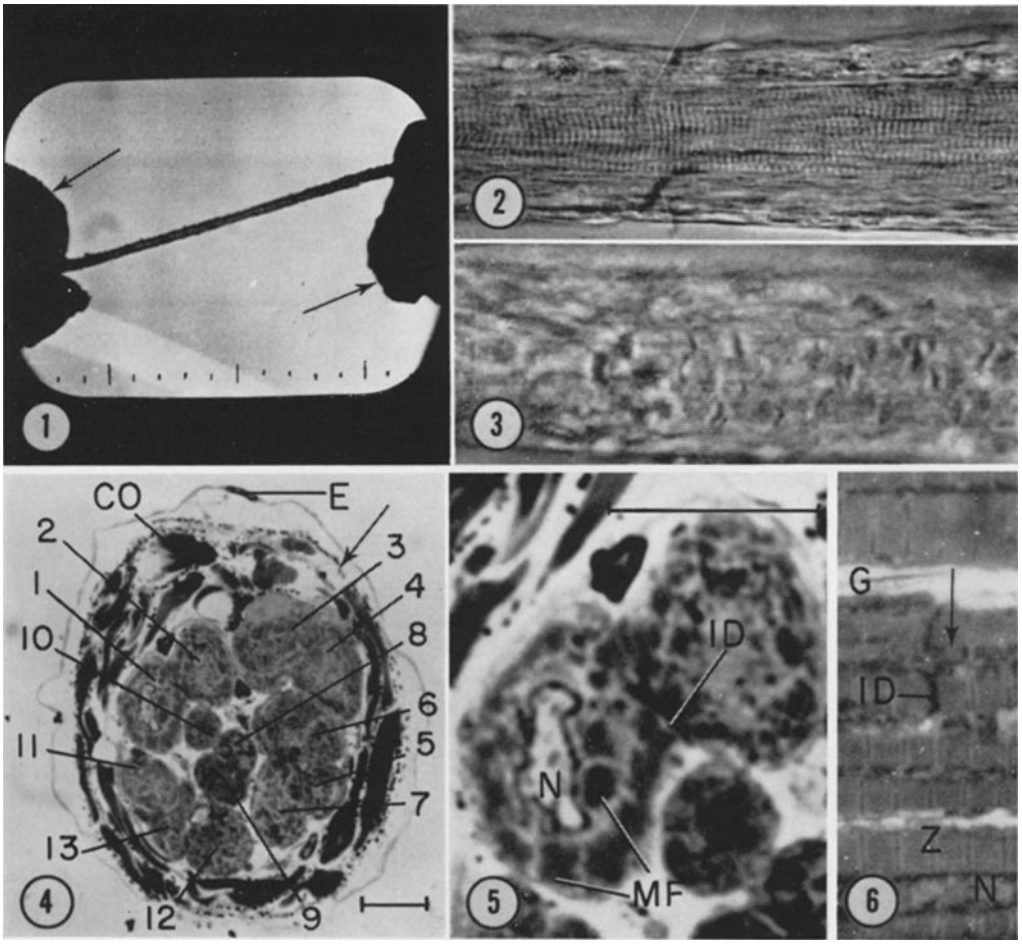

FIGURE 1 Low power photomicrograph of the basic preparation used in this investigation. The preparation is suspended between two lumps of ventricular muscle (arrows) that, in turn, are suspended between suction pipettes in a Krebs-Henseleit solution. × 30.

FIGURE 2 Higher power photomicrograph of a strand showing cross-striations, the type of preparation used in this investigation. × 425.

FIGURE 3 Higher power photomicrograph of a strand without visible striations, a kind of strand that was often encountered but not used in this study. × 715.

FIGURE 4 Transverse section through a strand stained with toluidin blue and observed with an oil immersion lens. The strand is surrounded by endocardium (*E*). Next comes a thick layer of collagen (*CO*) intermingled with fibrocytes and Schwann cells that contain axons and synaptic boutons (arrow). The fibers are numbered in the order in which they appear in Fig. 7. Thin sections adjacent to this thick section have been studied with the electron microscope (see text). The horizontal bar represents 10 μ. × 890.

FIGURE 5 High power photomicrograph of fibers *1* and *2* (cf. Fig. 4) to illustrate the central nucleus (*N*), the myofibrils (*MF*), and the junctional complex (*ID*) in the neck of the dumbbell-shaped profile formed by the two adjoining cells. The horizontal bar at the top of the figure represents 10 μ. × 2700.

FIGURE 6 High power photomicrograph of fibers of the strand cut longitudinally. One of the fibers is transected by a dark, thick wavy line, conventionally referred to as intercalated disc (*ID*) that connects two cells in longitudinal direction. The arrow points to a region in which the intercalated disc appears interrupted in longitudinal direction and where continuity of the myoplasm seems to exist. However, this region most likely represents a zonula occludens that usually connects cells in longitudinal direction and that is not visible in the light microscope. × 1700.

The heart was washed free of blood; the right ventricular wall was removed, by cutting along its septal border, and transferred to a tissue chamber perfused with Krebs-Henseleit solution at 37°C. Small "trabeculae carneae" (30–80 μ in diameter), hereafter referred to as "strand," were removed from the endocardial surface of the right ventricular wall by excising a small portion of the wall to which each end of the strand was attached. The strand was then held, just taut, between two small suction pipettes which were applied to the lumps of ventricular muscle at its ends (Fig. 1). The strand was examined microscopically with a water dipping 40×, 0.75 NA Zeiss phase objective with bright-field condenser at a final image magnification of 1,000. The image contrast was enhanced by appropriate use of a high resolution (800 lines horizontal) closed circuit television system. Viewed in this way, the strands were found to vary in the density and distribution of sarcomere striations. Some strands exhibited striations throughout most of (if not their entire) length and depth (Fig. 2), whereas others contained no visible striation (Fig. 3). The strands with striations, all of which contracted spontaneously or in response to electrical stimulation, were chosen for further microscopic examination as described in the paper, particularly since current electrophysiological and mechanical studies were confined to this kind of strand (Fig. 2).

B. *Papillary Muscle*

For the comparative studies on common ventricular muscle fibers, as opposed to the fibers of the strand, suitable papillary muscles were removed from the rabbit hearts and immediately fixed in glutaraldehyde (47) and processed as described below.

C. *Fixation and Preparation*

In order to provide further support for the strand during the exchange of fluids in fixation, we manipulated two glass rods under the strand and positioned them so as to support but not deform it. While the strand was still suspended between the two suction pipettes, the Krebs-Henseleit solution was rapidly replaced by 4% glutaraldehyde in 0.05 M phosphate buffer, pH 7.4, and the strand was fixed for approximately 30 min, a time that was sufficient to preserve the original straight configuration of the strand in subsequent steps. Suction was then released and the strand with its terminal lumps of muscle was transferred to a small test tube for further fixation in glutaraldehyde. At this point, it was necessary to cut off one of the lumps of muscle so that the strand would float freely and, thereby, maintain its straight configuration. If both lumps were left on the ends of the strand, the latter tended to sag and would be fixed in a curved position in the subsequent osmium tetroxide fixation. The time of fixation in glutaraldehyde mattered little and varied between 2 and 16 hr (refrigerated), depending on convenience only. Thereafter, the strands were washed in distilled water (with five changes) for 2 hr, whereupon the tissue was fixed in 1% osmium tetroxide in 0.05 M phosphate buffer for 2 hr and embedded in Maraglas (53). Maraglas was chosen in preference to Epon since, although there is no noticeable difference in the quality of embedding between the two media, Maraglas has the advantage that it can be easily straightened out in the water bath with xylol. Maraglas is also exceptionally stable in the beam even when the openings in the grid are only partially covered.

The strands were first embedded in low plastic dishes and, after polymerization, cut out from the hardened Maraglas, aligned in both horizontal and vertical directions (for longitudinal and transverse sectioning, respectively), and glued with Esterwax to Lucite blocks that fitted the Porter-Blum MT-1 ultramicrotome. Thick (approximately 1 μ) and thin sections were cut. The former were stained with toluidine blue, essentially according to the procedure of Richardson (42); the thin sections were stained with lead citrate (40), supported by naked 300-mesh copper grids, and viewed with an RCA EMU

FIGURE 7 Distribution of probable low resistance connections between fibers in a segment of the strand, determined from serial transverse sections. The numbers running horizontally denote the thirteen fibers, represented by the vertical lines, that were identified in the first section. The numbers running vertically denote the section (~1 μ thick). A horizontal line joining two (or more) vertical lines (beginning and ending with a solid dot) signifies that the two (or more) fibers are judged occluded with one another in that section. The heavy horizontal lines represent two (or more) horizontal lines. When a vertical line ends prematurely, this signifies that the fiber became attenuated and finally vanished. When a vertical line splits, e.g. No. *3* in section No. *18* splits into *3 a* and *3 b*, this indicates that the fiber split into two components (and vice versa). Only 162 of the 185 sections are shown.

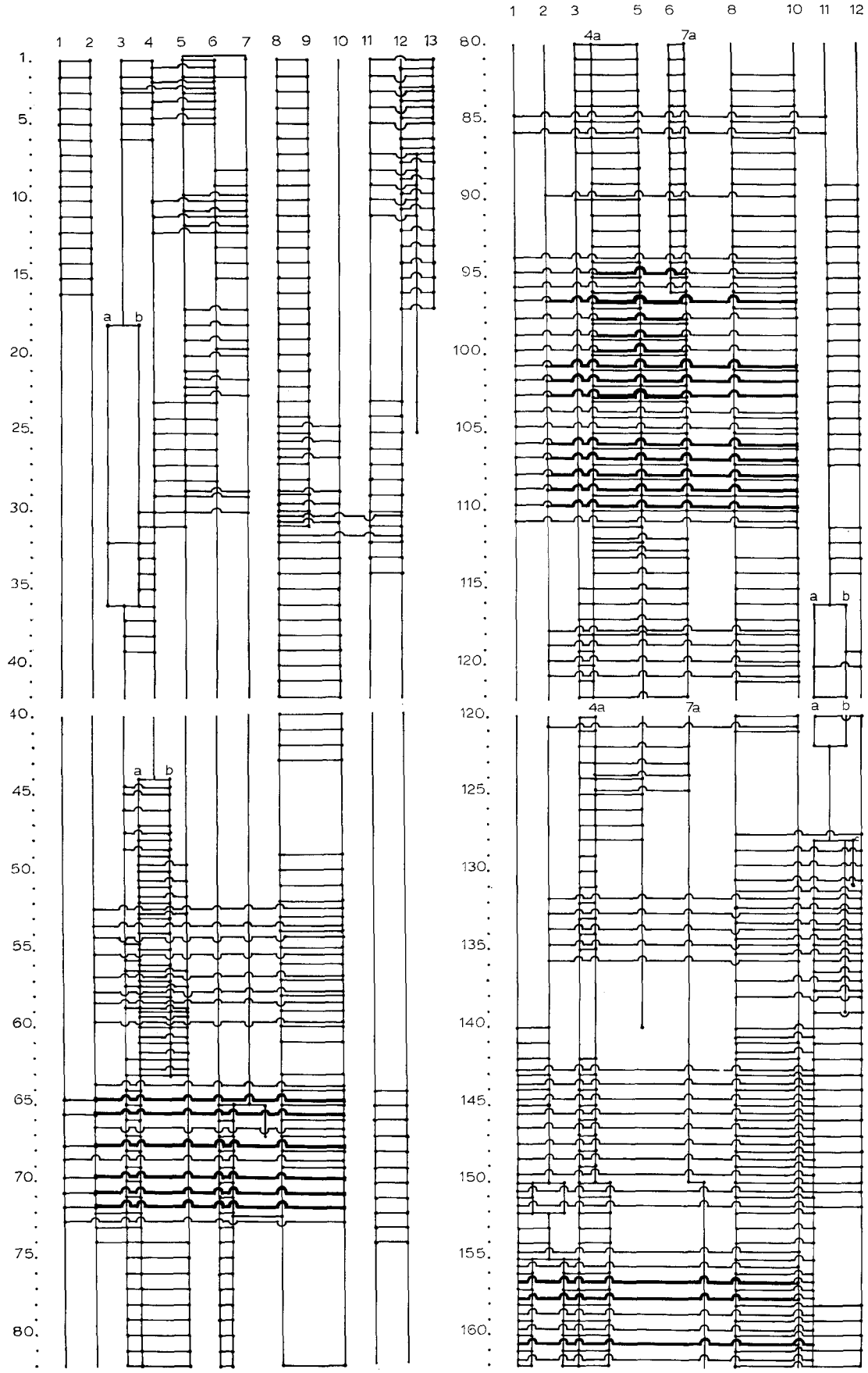
1 2 3 4 5 6 7 8 9 10 11 12 13
1.
5.
10.
15.
20.
25.
30.
35.
40.
a
b
40.
45.
50.
55.
60.
65.
70.
75.
80.
a
b
1 2 3 5 6 8 10 11 12
80.
85.
90.
95.
100.
105.
110.
115.
120.
4a
7a
a
b
120.
125.
130.
135.
140.
145.
150.
155.
160.
4a
7a
a
b
c

3-F at an accelerating voltage of 50 kv. Photographs were taken at original magnifications ranging from approximately 1300 to 32,000.

D. *Serial Sections*

Because of the length of the strand that was to be studied, thin serial sections were considered impractical. Therefore, part of the strand was cut transversely into 200 approximately 1-μ-thick consecutive sections which were put on glass slides and stained as above. Each of these sections was then photographed with a Leitz Automat attachment to the Leitz Ortholux microscope through an oil immersion phase objective 90 ×, NA 1.25, and Heine phase condenser, the light source being a Leitz mercury vapor lamp. Discs comprising the entire cross-section of the strand were cut out of the prints made of these photographs (Fig. 4). These discs were then roughly oriented with respect to a common transverse axis and longitudinal axis and mounted on a sheet of cardboard. The discs were fixed to the sheet, overlapping like shingles, with a small strip of adhesive tape that served as a hinge. In this way, the prints of successive serial sections could be easily examined and quickly compared. Although no perfect orientation was attempted, it was evident that the individual fibers followed a helical rather than a straight course relative to the longitudinal axis of the strand and to one another. Occasionally, a section was folded or otherwise distorted and could not be interpreted, but there were only eight of these and, in each instance, the adjacent sections were good.

Initially, in two different strands, a light- and electron-microscopic correlation was established of the appearance of regions of surface contact between adjacent muscle fibers. To this end, thick sections were cut followed by adjacent thin sections. Electron micrographs of the latter were taken at low and high magnifications, and composite pictures of the complete cross-section of a strand were assembled. The appearance was then compared with that of the adjacent thick section under the light microscope. Against the background of these direct comparisons between light and electron microscopic photographs, one could follow the individual fibers through the light-microscopic series and be reasonably certain of the nature of the fiber contact (see below). The individual muscle fibers in the photographs of the transverse sections were then numbered (Fig. 4) and traced individually through all thick sections. Since a wax model did not show the relationships between the fibers clearly, we decided to represent them in the form of a quasi-electrical wire diagram (cf. Fig. 7). In this diagram, we assume that the membrane structure of the zonula occludens (see below) presents a low electrical resistance compared to the sarcolemma. In the diagram the individual fibers are spread out on a plane, whereas actually they are arranged as a bundle (Fig. 4).

DEFINITIONS AND CRITERIA

A. *Fiber Contact*

When the serial light microscopic sections were analyzed and the character of contact between two fibers was described, only two distinctions were made, i.e. "open" or "occluded."

OPEN CONTACT: We judged the contact "open" when the fibers were totally separate in light microscopy. In these instances the adjacent electron micrographs always revealed both fibers to be surrounded by sarcolemma with its basement membrane. There remained a few instances in light microscopy in which the fibers touched, but actual occlusion was still in doubt. In such cases, the junctions in question were always considered to be "open." As it turned out, these questionable junctions invariably evolved into a unquestionable occlusion in the next few sections. Thus, it is important to note that the occlusions tabulated in the diagram (cf. Fig. 7) represent more the minimum of occluding contacts rather than the maximum.

OCCLUSION: Several articles have recently appeared in the literature which describe in detail the different cell junctions of various cells, including those of heart muscle cells (5, 9, 12, 13, 58, 44). The dimensions of the junctional membrane complexes are remarkably uniform, as described by different observers with different techniques and different cells. Various names have been given to these junctional membrane complexes. We are following the terminology of Farquhar and Palade (12). Consequently, in this communication the terms occluding or occlusion refer to cell junctions that are identical to the zonula occludens of Farquhar and Palade and the nexus of Dewey and Barr (9). It should be noted that the zonula occludens, per se, cannot be resolved by the light microscope. However, as electron micrographs of adjacent sections showed, the zonula occludens rarely occurred as such alone; rather, it always alternated with zonulae and maculae adherentes. Like those of the intercalated disc in heart muscle, the dimensions of the zonulae adherentes are such that they can be seen with the light microscope (Figs. 5, 6). Thus, it is by the almost invariable association with the zonula adherens that the presence of the zonula occludens can be estimated by light microscopic observations. Moreover, with

the electron microscope, several zonulae occludentes have been observed alone without an associated zonula adherens, whereas the reverse observation was exceedingly rare. Therefore, together with what has been said previously, these observations again suggest that the regions of occlusion between individual fibers were actually more than those shown in the diagram (Fig. 7).

B. *Couplings*

The terms triads, pentads, dyads, and diads designate the numerical relationship between terminal cisternae of the sarcoplasmic reticulum and the transverse tubule (4, 35, 38, 49), the latter, by definition, being an invariant component of these composite structures. Thus, neither of the terms, *sensu stricto*, applies to junctions, common in heart muscle, between terminal cisternae of the sarcoplasmic reticulum and the sarcolemmal envelope surrounding the whole muscle fiber. Clearly, the junction between one terminal cisterna of the sarcoplasmic reticulum and a portion of the sarcolemma constitutes a functional unit, its being immaterial whether the sarcolemma is that of a transverse tubule or that of the peripheral envelope of the muscle fiber. In this communication, this unit will be referred to as "coupling," and as "peripheral coupling" when special reference is to be made to its location at the periphery of the muscle fiber. The term triad is used when it applies *sensu stricto*.

C. *Tubular Fibrils*

Tubular fibrils, the microtubules of Ledbetter and Porter (28), have been described in a great variety of cells of living organisms high and low on the phylogenetic scale (37, 7). They are, as a group, usually associated with regions in a cell that are mechanically important (flagella, mitotic spindles, cell junctions, cell wall pseudopods), and they have been shown to be capable of directional growth (52). Without entering into the controversy as to whether or not these structures are actually solid or hollow, we shall, for purely descriptive reasons, treat them here as tubular structures with a wall.

D. *Sarcoplasmic Reticulum*

It is realized that the sarcoplasmic reticulum is not necessarily represented by tubules but, rather, may be composed of interconnecting cisternae. In this communication, the sarcoplasmic reticulum is described in terms of tubules, and the term cisterna is reserved for that portion of the sarcoplasmic reticulum which is part of the couplings (see above).

RESULTS

A. *Light Microscopic Observations*

The strand was surrounded by a single layer of endothelium (endocardium) (Fig. 4). Abundant bundles and fibers of collagen were arranged both longitudinally and transversely to the axis of the strand, and pervaded the endomysium between the muscle fibers. Between the collagen fibers, a number of fibrocytes and Schwann cells of the autonomic terminal reticulum were seen. Both cell types cannot be distinguished in light microscopy, but the boutons of the autonomic nerve fibers were visible as small blue dots among the collagen fibers (Fig. 4).

At this level of resolution, the muscle fibers proper were indistinguishable from common ventricular muscle fibers as regards their contractile behavior, striations, and the presence of intercalated discs. The myofibrils of the strand, within limits of considerable variations, showed some slight preference of position with respect to the periphery of the cells (Figs. 4, 5). Most muscle fibers seemed to have only one nucleus in the center of the cell (Figs. 5, 6). The myofibrils were surrounded by sarcoplasm which contained varying amounts of glycogen. The individual fibers were separated by endomysium, except where two or more appeared to fuse with one another, in which case a dark, frequently broken and very thick wavy line was often demonstrable (Figs. 4, 5) which corresponded to the intercalated disc, or zonula adherens, as seen in longitudinal sections (Fig. 6). The presence of such a structure was always interpreted as occlusion between two fibers. Fibers, thus occluded, almost always formed a dumbbell-shaped profile, the occlusion occurring in its neck (Fig. 5). This was also the place in which the cells would separate in subsequent sections. In some instances, the dark line was very small and, on either or just one end of it, the two adjacent cells occasionally presented areas of apparent continuity (Fig. 6), which presumably represented occluding zonules. That such regions of apparent cell continuity were, in fact, zones of unresolved close cell apposition, often became clear

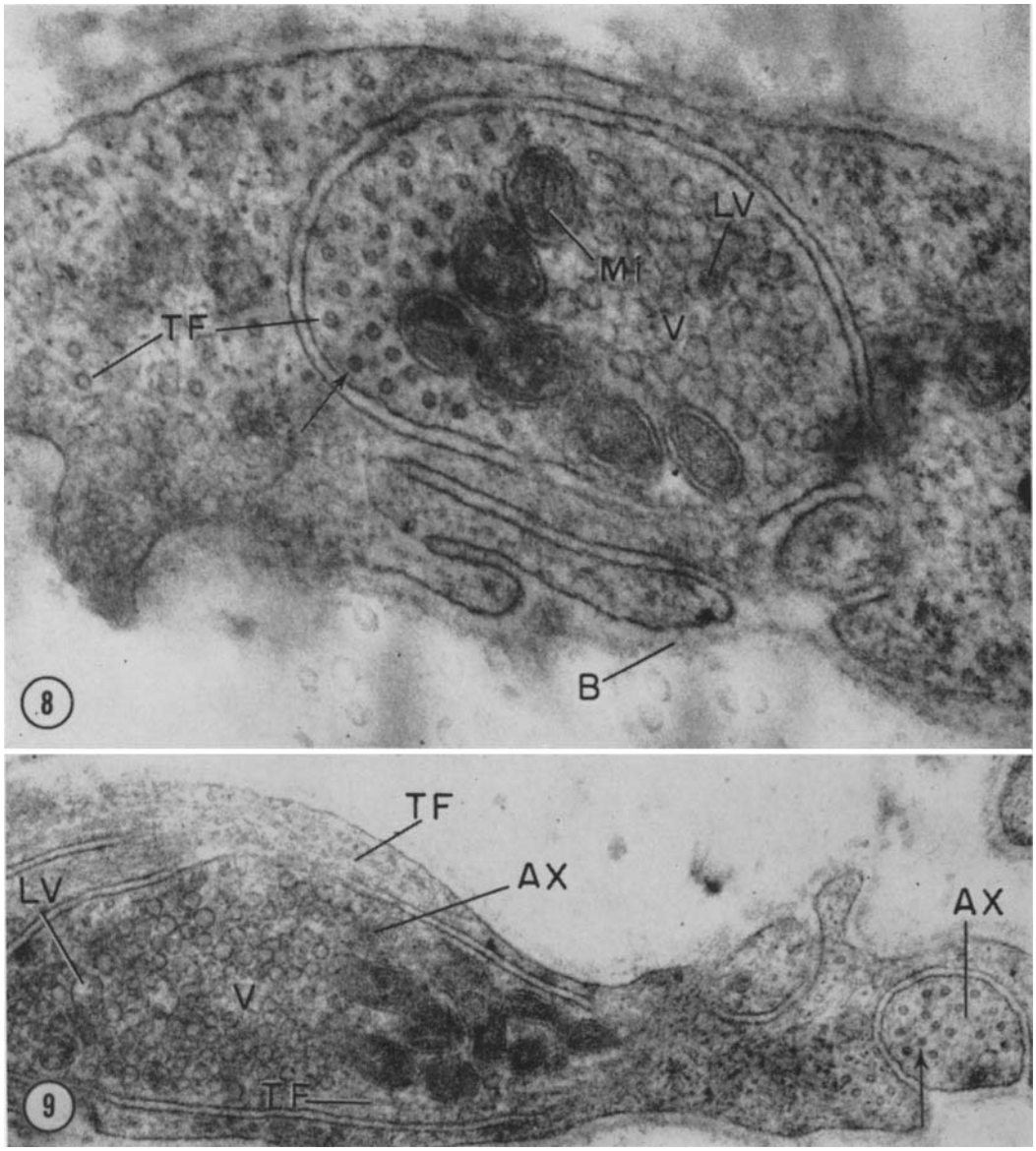

FIGURE 8 Strand. Schwann cell with its characteristic basement membrane (*B*), and an axon showing synaptic vesicles (*V*), mitochondria (*Mi*) and tubular fibrils (*TF*). The arrow points to a tubular fibril with a dense core (cf. Fig. 9). Note absence of dense core in tubular fibrils in the cytoplasm of the Schwann cell. The synaptic vesicles (*V*) are rather uniform in size, except for a few that also may contain a dense nucleoid (*LV*). × 67,000.

FIGURE 9 Strand. Two axons in a Schwann cell. Tubular fibrils (*TF*) are present in the axons cut transversely and longitudinally. The arrow points to the central core in one of the tubular fibrils. Note absence of central core in tubular fibrils in the cytoplasm of the Schwann cell. Larger vesicle (*LV*). × 29,000.

when these two cells separated in that plane in subsequent serial sections.

B. *Electron Microscopic Findings*

1. Nonmuscular Components

The strands under investigation (30–80 μ in diameter) contained no blood vessels. The endothelial cells of the endocardium and the fibrocytes and the Schwann cells of the autonomic nervous system were no different from those described in the literature. Whereas some strands were completely pervaded by numerous autonomic nerve fibers, other strands had only a few. The nerve fibers had numerous boutons along the course of the axons. Muscle fibers adjacent to closely apposed boutons often contained large accumulations of "pinocytotic vesicles" and mitochondria, but densities in the sarcolemma such as have been described by Page (34) were not seen. The vesicles of the synaptic boutons were usually uniform in size, although a few larger ones were always present (Figs. 8, 9). The latter sometimes contained a dense nucleoid in the center (Fig. 8), which may be indicative of a catecholamine content (18). Mitochondria were always present, as were tubular fibrils running parallel to the axis of the axon. On transverse section, the tubular fibrils measured approximately 25 mμ over-all diameter and the wall measured approximately 6 mμ. Tubular fibrils of similar dimensions were also seen in the cytoplasm of the Schwann cell (Figs. 8, 9). However, the tubular fibrils in the axon usually displayed a dense core in the center of the fibril, whereas those in the cytoplasm of the Schwann cell did not (Figs. 8, 9). Similar nerve fibers were also seen occasionally in the papillary muscle of the rabbit.

2. Muscle Fibers of the Strand

a. GENERAL OBSERVATIONS: The fibers of the strand were surrounded by sarcolemma with its basement membrane (Fig. 10) and had innumerable subsarcolemmal "pinocytotic" vesicles. Collagen fibrils were always present, even in very small intercellular spaces. The muscle fibers varied somewhat in their content of both mitochondria and myofibrils. The number of nuclei per cell could not be determined. The nuclei frequently were indented by deep but narrow cytoplasmic invaginations which, in suitable sections, may give the impression that the cell is multinucleated. Here and there, but infrequently, a conglomeration of vesicles was found, intermixed with an occasional mitochondrion and myelin figure. Identical structures were present in the papillary muscle, and sometimes the impression was gained that they, perhaps, belonged to Golgi complexes.

b. MYOFIBRILS: In material prepared for electron microscopy, no attempts were made to measure the resting sarcomere length. Judging from light microscopic measurements of living muscle, that resting length was close to 2 μ (25). So far, it has not been possible to determine unequivocably whether or not an H zone appears when the fibers are stretched. Because of the large parallel elastic component (collagen) in the strand, uniform stretching of the fibers in the strand to a length suitable for demonstrating an H zone is very difficult. In all other respects, the sarcomeres displayed the usual structure and dimensions characteristic of those in the common ventricular fibers of the papillary muscle (Figs. 11–13). They had M lines, Z lines, A and I bands. In contrast to those in slow muscle (21), the Z lines were usually straight, as in twitch muscle, but were occasionally broken up into several smaller fragments (Fig. 11).

c. CELL JUNCTIONS: The following forms of cell junction were found both in the strand and in papillary muscle (Fig. 14):

1. The zonula adherens, e.g. the "zigzag" portion of the intercalated disc seen in longitudinal sections.
2. The macula adherens, the desmosome.
3. The zonula occludens, e.g. the nexus or tight junction, the longitudinal portion of the intercalated disc. No attempt was made to define, by serial sections, maculae occludentes.

As has already been mentioned, the zonulae adherentes, almost without exception, were associated with zonulae occludentes. Since the zonula occludens, in heart muscle, is longitudinally oriented, it was only in the transverse section that the extent of this type of cell junction could be evaluated. Zonulae occludentes as long as 10 μ in one dimension have been observed (Fig. 15). Most frequently the whole junctional complex between two cells was composed of all three forms of close contact, i.e. zonula occludens, zonula adherens, and macula adherens (Figs. 16, 17). Although there did not seem to be any particular sequential order among the junctions, a zonula occludens or a macula adherens, commonly, but not always,

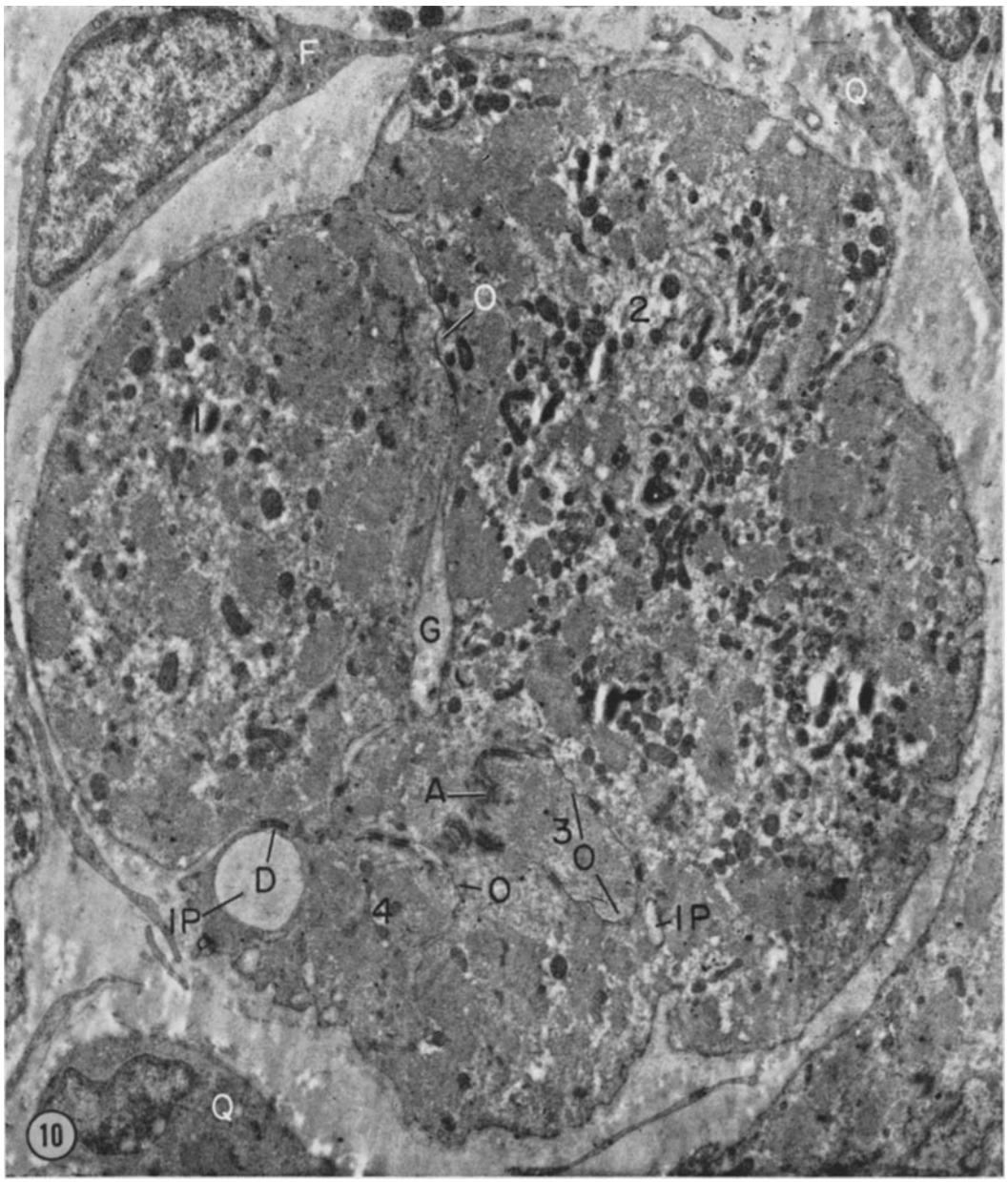

FIGURE 10 Transverse section of one "fiber" (cf., for example, fiber *10* in Fig. 4) which is separated into four (*1*, *2*, *3*, *4*) components by junctional complexes. Note zonula occludens (*O*), zonula adherens (*A*), and *macula adherens* (*D*). The fibrocyte (*F*) and the Schwann cells (*Q*) are distinguished by the absence and presence of a basement membrane, respectively. *IP*, inpouching of extracellular space. × 9500.

was the first junction toward the larger extracellular space (Figs. 16, 17).

The large extent of lateral connections between muscle fibers could be appreciated in longitudinal sections (Figs. 15, 19). For the most part, these connections were detectable by light microscopy, whereas many other, smaller ones, clearly were not (Figs. 18, 20). In studying the serial sections of

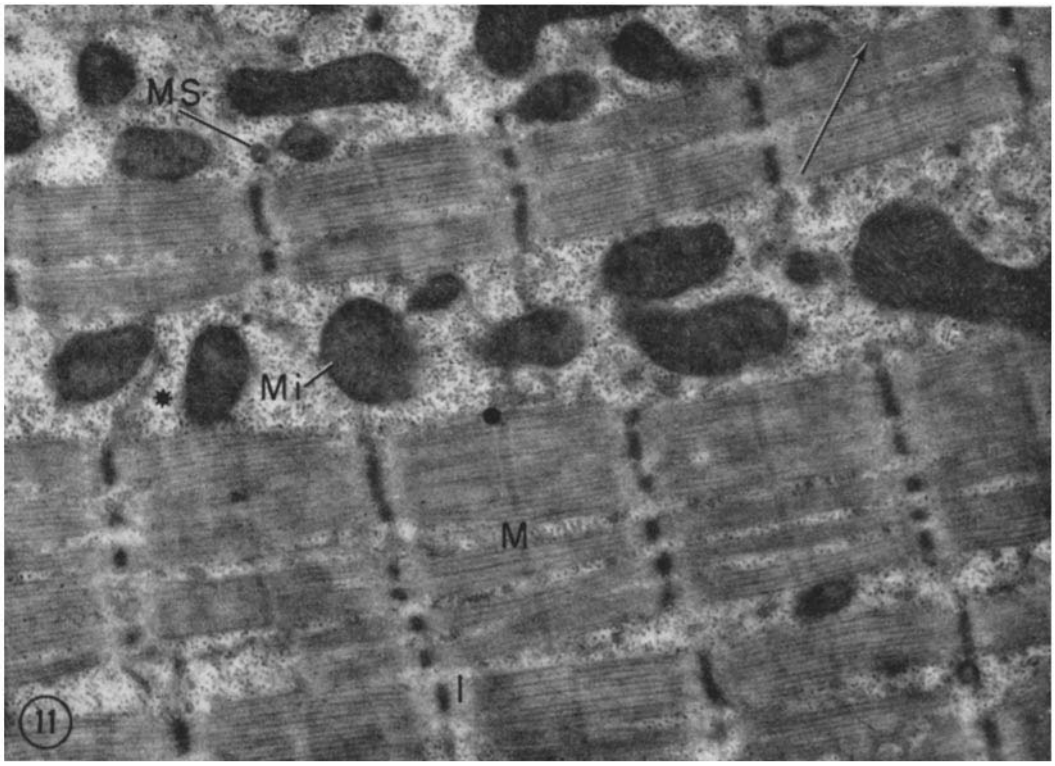

FIGURE 11 Strand. Typical sample of general topographic relationships between myofibrils and the sparse tubular system in the sarcoplasm (cf. Figs. 26–30). Note converging tubules at *M* line (arrow), tubular connection between Z line and M line (star), and mitochondrion with one central crista (*MS*). The remaining mitochondria (*Mi*) are similar to those seen in papillary muscle. The sarcomeres show I bands (*I*), particularly when stretched, and M lines (*M*) and Z lines. The latter often are broken up into fragments but are straight when fused (cf. Figs. 33–37). × 22,500.

1-μ thickness with light microscopy, it was often noted that an "occlusion" turned into an "open contact" (see Definitions and Criteria) for as little as one or two sections (approximately 1–2 μ), only to become "occluded" again in the following sections. These observations find their ready explanation in the regions marked *G* in Fig. 19, which demonstrate the opening up of junctional complexes over short distances. In the same figure, a junctional complex is seen to run obliquely to the long axis of the two adjoining fibers (long arrow). At some distance beyond the upper limit of the illustration one of the two fibers may be presumed to become extremely attenuated, only to disappear altogether (cf., e.g., Fig. 7: fiber *6*, section *96*). The transverse section of the junctional complex of two such fibers is shown in Fig. 17. One of the fibers is attenuated to the point that it merges imperceptibly with the general circumferential contour of the remaining larger fiber. Fig. 10 serves to illustrate further the fusion by juctional complexes of several fibers. In this figure, the fiber which looks like a single fiber (cf., e.g., fiber *10* in Fig. 4) surrounded by endomysium was found to be composed of what appear to be four fibers (labeled *1–4*) which can be distinguished by following the junctional complexes (*o* in Fig. 10). Finally, some fibers were connected by only a zonula occludens (Figs. 18, 20).

d. COUPLINGS AND SARCOPLASMIC RETICULUM: In contrast to papillary muscle (Figs. 12, 13), the strand did not have any triads. However, peripheral couplings were common. The morphological features of the couplings of both the strand (Figs. 21, 22, 24, and 25) and the papillary muscle (Fig. 23) were identical. One of the components of the coupling consisted of a cisterna of the sarcoplasmic reticulum, bounded

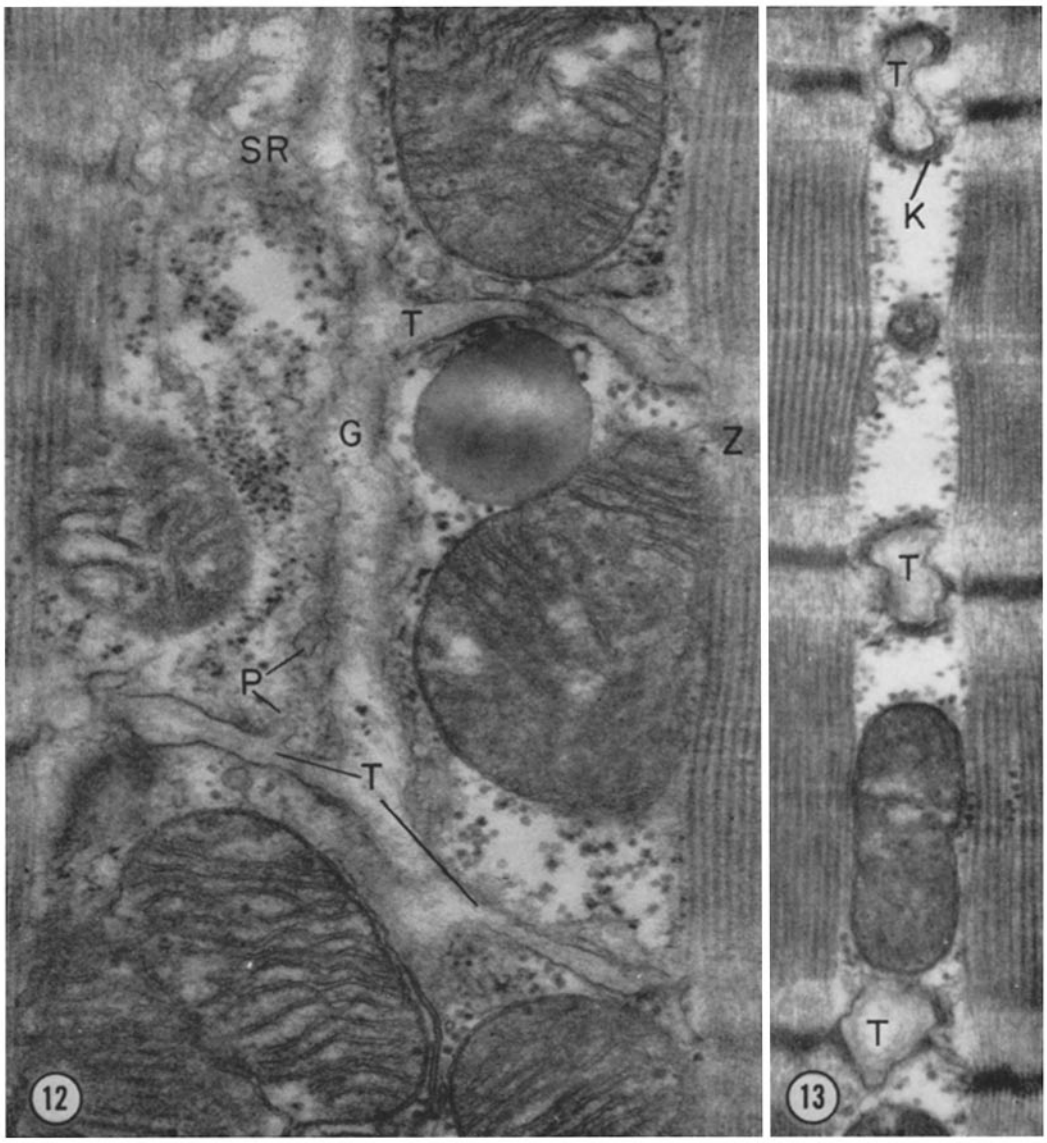

FIGURE 12 Papillary muscle. Three transverse tubules (*T*), complete with basement membrane, extending from the intercellular space (*G*) to Z lines (*Z*). Note sarcoplasmic reticulum (*SR*) and "pinocytotic" vesicles (*P*). × 53,500.

FIGURE 13 Papillary muscle. Transverse section of three triads, each formed by a transverse tubule (*T*) and two terminal cisternae of the sarcoplasmic reticulum (*K*). × 39,000.

by a membrane of unit membrane configuration (43). In the center of the cisterna and running parallel to its long axis there was a dense, often broken, and sometimes wavy line with a thickness slightly less than that of the membrane enveloping the cisterna. In the papillary muscle this central broken line was seen only in couplings. In the strand it was seen occasionally in short stretches of tubules that, apparently, were not in junction with the sarcolemma (Figs. 21, 24, 28), though it is impossible to rule out apposition of sarcolemma outside the plane of sectioning. Usually, however, the

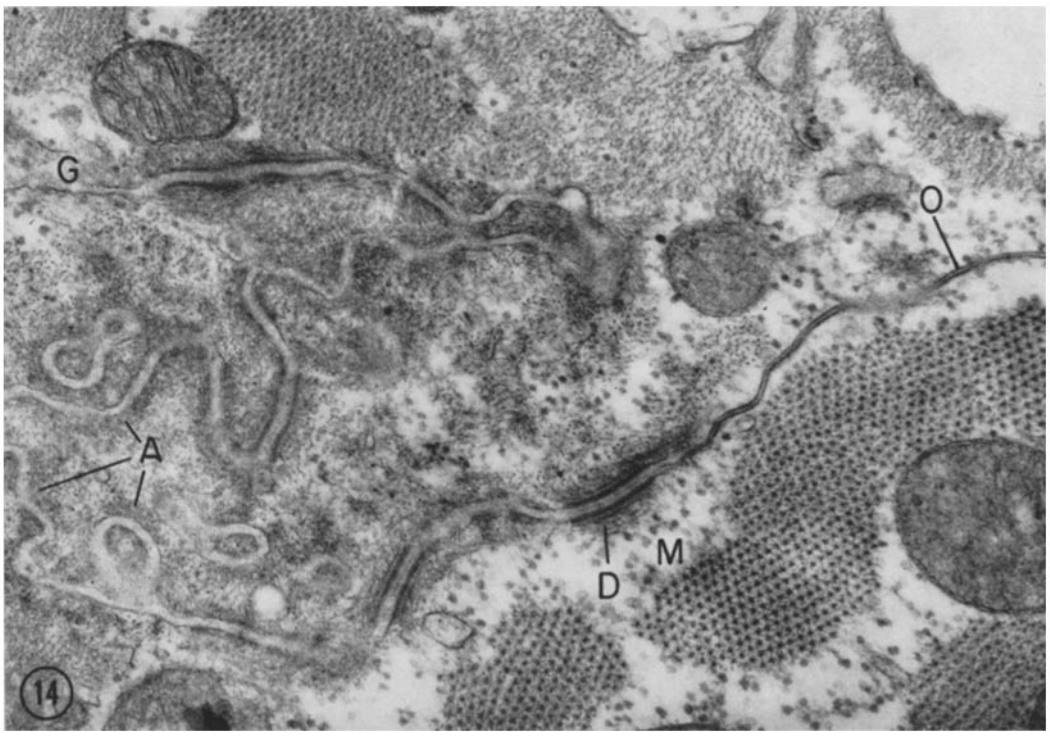

FIGURE 14 Section to illustrate the three kinds of cellular apposition, found in both the strand and the papillary muscle: z. adherens (*A*), z. occludens (*O*), and m. adherens (*D*). G, intercellular space; *M*, M line. × 68,500.

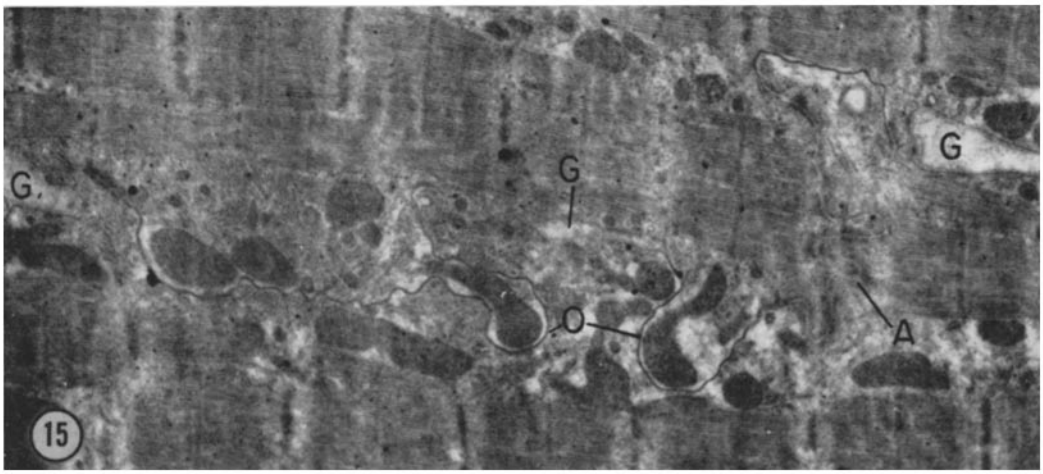

FIGURE 15 Strand. Longitudinal junctional complex between two fibers, revealing the characteristic orientation of the z. occludens (*O*) with respect to the longitudinal axis of the sarcomeres and in relationship to the transverse portion of the intercalated disc, the z. adherens (*A*). Note the intimate association of the z. occludens with mitochondria, a rather consistent relationship. × 16,500.

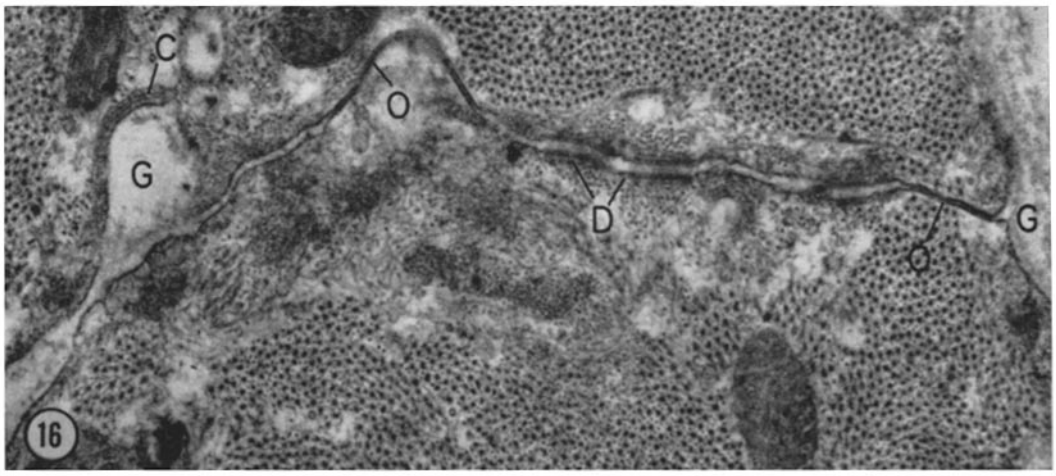

FIGURE 16 Strand. Typical junctional complex between two fibers, which begins with a z. occludens (*O*) on each side, with m. adherentes (*D*) in between. *C*, peripheral coupling. × 52,000.

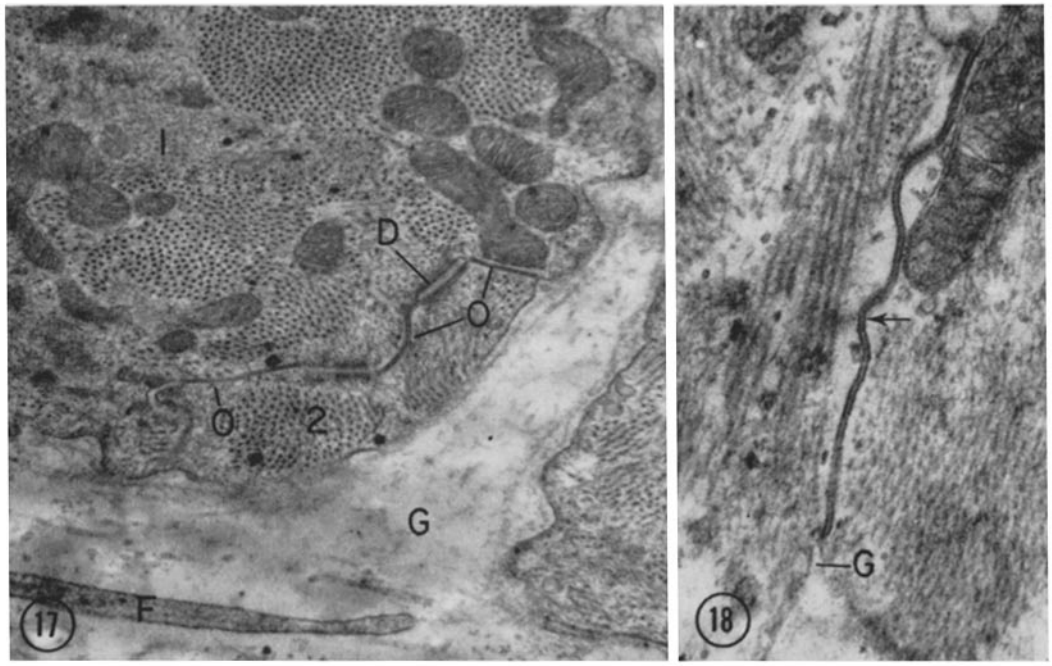

FIGURE 17 Strand. Transverse section through a large fiber (*1*) and a small fiber (*2*). Fiber *2* has fused smoothly with the general contour of fiber *1*. From serial sections, it is clear that fibers like fiber *2* represent the attenuated end of a fiber that, ultimately, loses its identity (cf. fiber No. *6*, serial section No. *96* of Fig. 7). Note z. occludens terminating the junctional complex on either side. × 21,500.

FIGURE 18 Strand. Two cells apposed in the typical dumbbell-shaped fashion (cf. Fig. *5*) with only a z. occludens forming the junction. Arrow points to central density between the junctional membranes. × 42,000.

central broken line in the cisternae of the couplings extended only over the length of the coupling (Figs. 23–25), that is to say, over the length of intimate contact between the terminal cisterna and the sarcolemma. Granular material was never seen within the terminal cisternae of either the fibers of the strand or of the papillary muscle. That portion of the cisternal membrane that was closest to the sarcolemma appeared to have regularly spaced (approximately 40 mμ from center to center) processes extending toward the sarcolemma (Figs. 22, 23). These processes (approximately 20 mμ in width) seemed to be outpouchings of the cisternal membrane and appeared to fuse with the sarcolemma, in some but not all instances. The sarcolemmal component of the couplings was structurally indistinguishable from other portions of the sarcolemma, though sometimes a small dent occurred just opposite one of the processes of the cisterna (Fig. 22, long arrow). Couplings never occurred at a zonula occludens, zonula adherens, or macula adherens.

As in papillary muscle (Fig. 12), networks of interconnecting tubules in the sarcoplasm were infrequent. When present, they were usually at a Z line (Figs. 27, 30). For the most part, the sarcoplasm was pervaded by single, though branching, tubules that were of varying diameters, ranging between approximately 30 and 50 mμ (Figs. 11, 26–30). Many of the tubules were associated with Z lines and M lines and could be observed traversing the interfibrillary space transversely, usually from Z line to Z line (Fig. 29) but also from Z line to M line (Fig. 11). Branching of these tubules into a transverse component and a longitudinal component was observed (Figs. 26, 30). Frequently, two such tubules converged upon a Z line or M line (Fig. 11, arrow; Fig. 29, *a*). The cisternae of the peripheral couplings were continuous with these tubules (Fig. 21). The central dense line, a characteristic morphological feature of the couplings, was occasionally seen inside a tubule at the Z line (Fig. 28). In none of the tubules in the sarcoplasm was the lumen seen to be continuous with the extracellular space. However, in one instance the cisternal component of a coupling seemed to be continuous with a pinocytotic vesicle that, in turn, was open to the extracellular space. Following the procedure of Huxley (22), we could not demonstrate ferritin in any of the tubular components of the sarcoplasm, though it was present in the endomysium. It would seem, however, that negative findings obtained with the ferritin may not be so conclusive as positive ones would have been. However, it will be recalled that the strand is surrounded by endocardium and a considerable layer of collagen. In a 30- to 80-μ strand, it is impossible to split the envelope so as to provide the ferritin easy access to the fibers. As a result, and without resorting to forced injection, one is restricted to allowing the ferritin, which has a large molecular weight, to diffuse in longitudinal direction from the cut ends of the strand. It is felt that further work is required to clarify this issue without equivocation.

Very rarely a tubule studded with ribosomes was encountered.

e. MITOCHONDRIA: Abundant mitochondria were present in all fibers of the strand. Sometimes they formed large irregular clusters (Figs. 10, 19), but more frequently were located between the myofibrils in a characteristic manner for cardiac muscle. As an invariant feature of the strand, two different kinds of mitochondria could be distinguished. One of them was very similar to the kind of mitochondria found in papillary muscle. The other was similar to the kind found only in nerve axons. These mitochondria were characterized by their length (up to 6 μ), their small transverse diameter, and the paucity of cristae (Figs. 31, 32; cf. Figs. 8–11, 19). In fact, most of them possessed only one central crista extending parallel to the long axis of the organelle (Figs. 31, 32). As a result, on cross-section they appeared doughnut-shaped (Fig. 11). One end of these mitochondria very often was in close proximity to a Z line (Fig. 31). In the matrix of many mitochondria of both kinds a central, sometimes broken line, reminiscent of that associated with the couplings, was observed.

f. PRESUMPTIVE SARCOMERES: In longitudinal sections of both the strand and the papillary muscle, very dense striae were seen emanating at right angles from the sarcolemma into the cytoplasm (Figs. 19, 33–37), approximately 0.1–0.2 μ deep. The spacing between the striae was regular (approximately 0.1–0.15 μ), and their appearance as well as their association with adjacent myofilaments suggests that they are related to Z lines. Connecting the striae were fine filaments of a thickness corresponding to that of actin filaments (Fig. 33). Sometimes striae appeared to be split by sharp invaginations of the sarcolemma (Figs. 34, 36), suggesting a possible early step in the morphogenesis of the striae. The striae almost always were arranged in the form of an arch be-

tween the two adjacent Z lines (Figs. 34–36), the top of the arch being at the level of the M line. From Fig. 35 it can easily be imagined how appositional growth of sarcomeres might be effected when, on both sides of the arch, striae are added to the shoulders (the existing Z lines) while, simultaneously, the myofilaments expand. The striae seemed to fuse, one by one, to form a continuous Z line, though this process may be retarded in some instances (see broken Z line in Figs. 11 and 35). Frequently, tubules of the sarcoplasmic reticulum were seen in contact with the striae (Figs. 33, 34).

DISCUSSION

Before discussing the electrophysiological implications of the interconnections between the individual fibers of the strand, it will be necessary to discuss some of the structural features of the strand.

It is clear that there are at least two different populations of muscle fibers in the rabbit right ventricle. One is found in papillary muscle, which presumably exemplifies the majority of ventricular fibers, and the other is found in the strand. The two populations are distinguished from one another, in that the fibers in the strand have no triads and have a kind of mitochondrion not found in papillary muscle. Other than on the basis of these two criteria, the fibers in the strand are difficult to distinguish from those of papillary muscle, for they are rich in myofibrils and contract spontaneously or in response to an electrical stimulus. On the basis of their location, the fibers of the strand may be categorized as Purkinje fibers. The latter have been the subject of numerous anatomical studies that were reviewed by Truex (54), but the light microscopic criteria for Purkinje fibers are uncertain, at best, especially in the rabbit. Recent electron microscopic studies (6, 26, 30, 41, 56) have not contributed additional criteria for their definitive identification, except, perhaps, the finding of small mitochondria with fewer cristae (26, 56) and the unusually large number of desmosomes observed in the steer heart (41).

One of the features characteristic of the fibers of the strand and, at once, one of the most significant findings of this investigation was the absence of triads, which was in sharp contrast to the abundance of triads in the common ventricular fibers of the papillary muscle (Figs. 12, 13). As has already been mentioned, the absence of triads or, for that matter, diads, implies the absence of transverse tubules. In fact, we found no evidence of a transverse tubular system that was continuous with the extracellular space. Ferritin was not demonstrable in the intracellular tubules. Even if, for reasons already mentioned, one disregards the latter observation, the following considerations suggest, independently, that there is only one tubular system within the fibers of the strand, namely the sarcoplasmic reticulum.

With ferritin as a marker, the recent investigations by Page have uncovered transverse tubules in slow muscle fibers that previously had been thought to lack them (34). It should be noted, however, that, even without the marker, Page did show convincing illustrations of triadic structures, although such triads were said to have been very infrequent. Page also noted, with respect to tubule size, two populations of tubules; one of them, comprising the smaller tubules, was predominantly oriented in a transverse direction, connecting Z lines. In the strand, however, we found only one population of tubules, although its constituents displayed some individual variations in their dimensions. Nevertheless, many of the tubules were distinctly oriented in a transverse direction, traversing the interfibrillary space from Z line to Z line or Z line to M line (Figs. 11, 29). This, at first, suggested that, perhaps, there was a trans-

FIGURE 19 Strand. Composite longitudinal section illustrating lateral connections between the fibers of the strand. The arrow in the left upper corner emphasizes the oblique course of some of the lateral junctions that may lead to the attenuation of one of the fibers until it completely disappears (cf. Fig. 17). The junctional complexes are interrupted by small segments of intercellular space (*G*) that were also frequently observed in the 1-μ serial transverse sections. Note striae (*St*) and the typical appearance of the classical intercalated disc (*ID*) which corresponds to its light microscopic morphology as shown in Fig. 6. × 7,800.

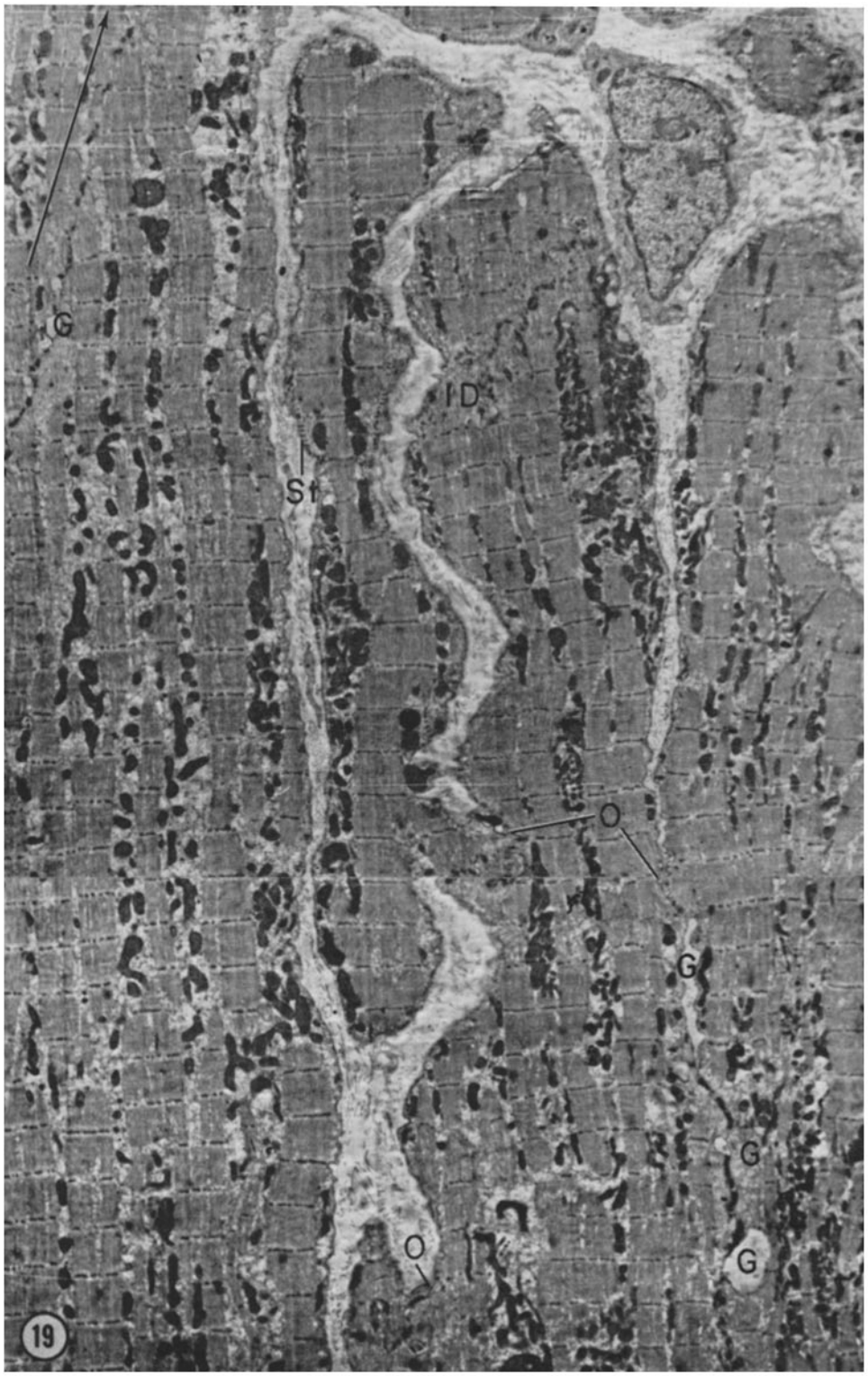
G
ID
St
O
G
G
G
O
G
19

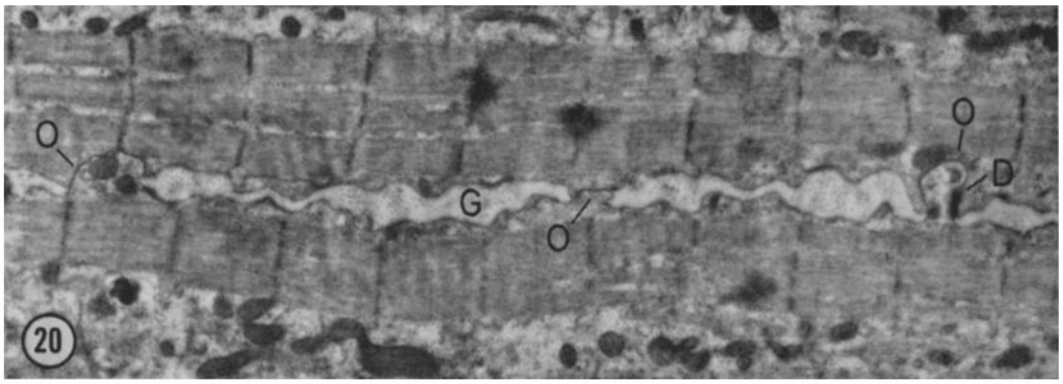

FIGURE 20 Strand. Longitudinal section of two adjacent fibers illustrating three very small z. occludentes (*O*), within a short distance from one another, which would escape recognition in the light microscope. × 10,800.

verse tubular system, *sensu stricto*. It was not until a direct connection was discovered between a peripheral coupling and a transversely oriented tubule at the Z line (Fig. 21) that the true nature of the intracellular tubular system became apparent. The structural details of the couplings were discrete, constant, and observed in the fibers of both the strand and the papillary muscle. There is no doubt that the terminal cisternae of the triads, as well as those in the periphery of the fibers

FIGURE 21 Strand. A peripheral coupling (*C*) is continuous with one of the two tubules converging upon a Z line (*Z* and arrows, cf. Figs. 11, 28, 29). Note central membrane (*CM*) in the coupling, but also in a segment of the tubule that is apparently away from the sarcolemma. Usually, the central membrane disappears as the tubule parts from the coupling (cf. Figs. 23, 24 (*SR*), 25). × 66,500.

FIGURE 22 Strand, transverse section. Two couplings (*C*) around an occasional inpouching of the sarcolemma (cf. Fig. 10 (*IP*)). The coupling (*C*) consists of a cisterna (*K*) of the sarcoplasmic reticulum, a central membrane (*CM*), cisternal processes (arrows and arrow heads directed downwards) and that portion of the sarcolemma that covers the processes. The regularly spaced processes appear as evaginations of the membranous envelope of the cisterna. Sometimes, they seem to fuse with the sarcolemma (long downward directed arrow); sometimes they do not (adjacent short arrow). The sarcolemma at the downward directed long arrow shows a small dent toward the adjacent cisternal process. × 67,000.

FIGURE 23 Papillary muscle, longitudinal section. The coupling (*C*) at the transverse tubule (*T*) is similar to the ones in Fig. 22. The terminal cisterna (*K*) of the coupling (*C*) is dilated beyond the termination of the central membrane (*CM*). The two arrows and the arrowhead emphasize the spacing of the cisternal processes. At the point of the long arrow, the cisternal process appears fused with the sarcolemma; the process at the arrowhead does not. × 82,000.

FIGURE 24 Strand. The central membrane (*CM*) of the coupling commonly disappears as the membranous envelope of the sarcoplasmic reticulum (*SR*) moves away from the sarcolemma and continues on toward a Z line (cf. Figs. 23, 25). Note the faint though distinct densities between cisternal envelope and sarcolemma corresponding to the cisternal processes (cf. Figs. 22, 23). × 74,500.

FIGURE 25 Strand. A small lateral junction by a z. occludens (*O*) only (higher magnification from Fig. 20). The cisterna of the sarcoplasmic reticulum loses its central membrane as it leaves the coupling (*C*). × 52,000.

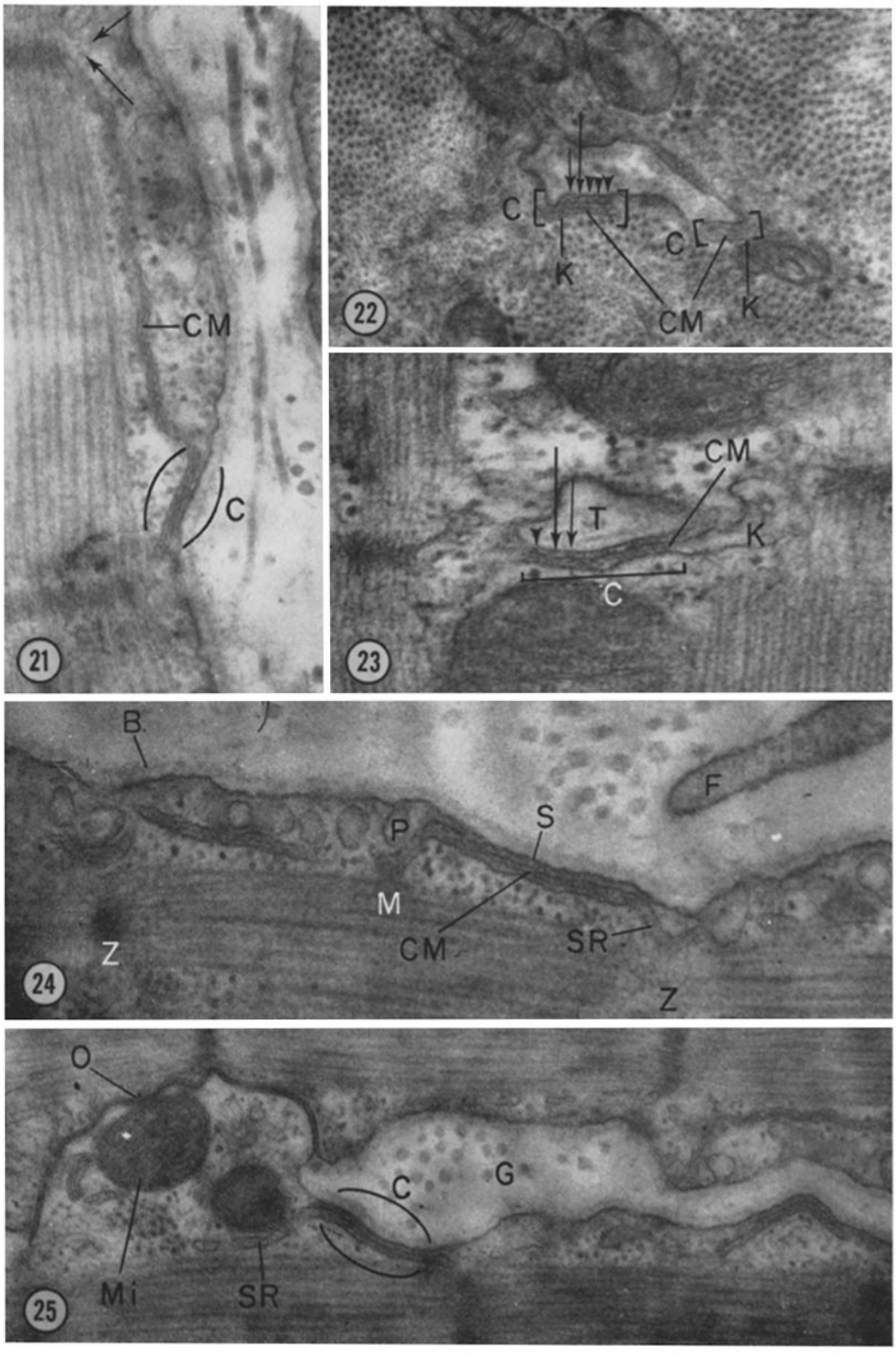
CM
C
21
C
K
CM
K
22
CM
T
K
C
23
B.
F
P
S
M
CM
SR
Z
Z
24
O
C
G
Mi
SR
25

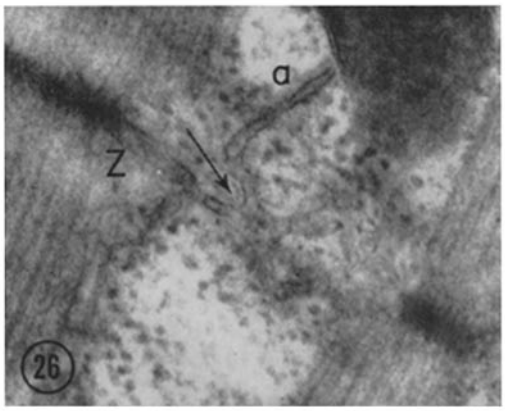

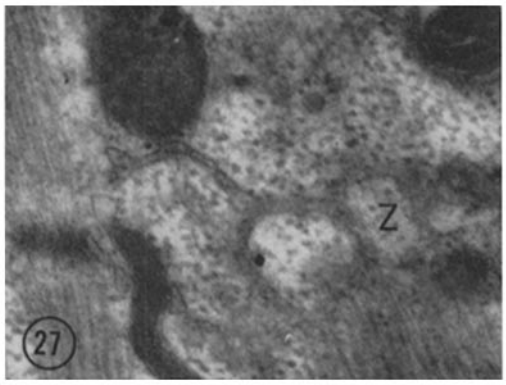

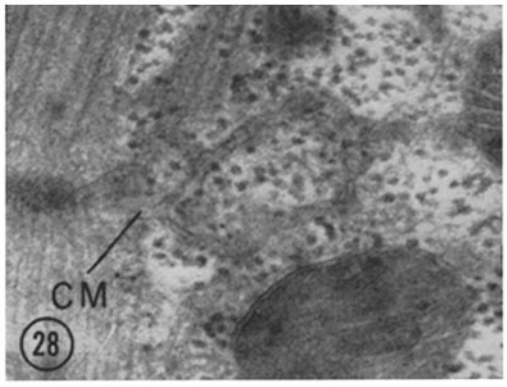

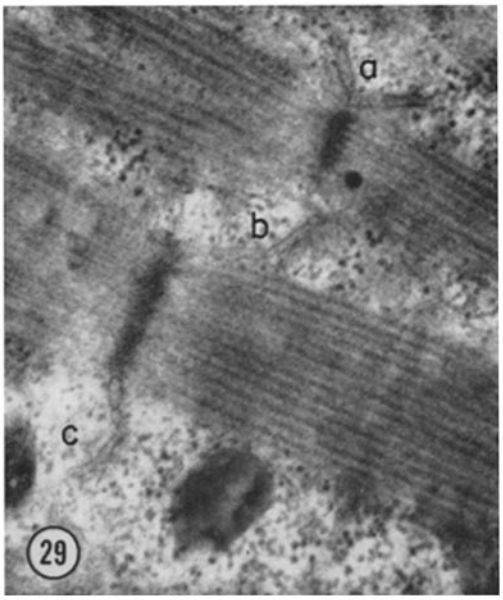

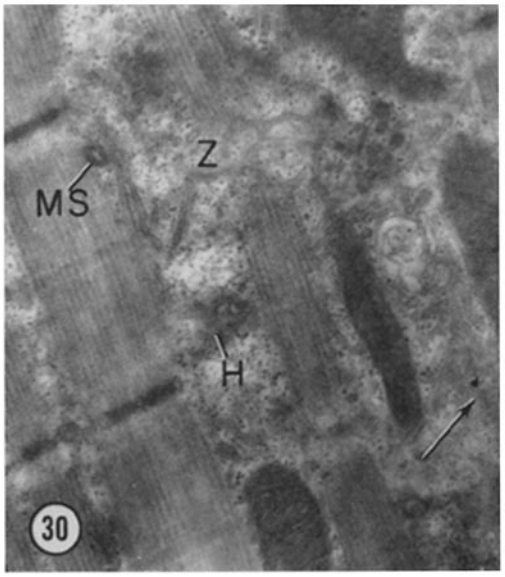

FIGURES 26–30 These figures illustrate the most characteristic appearance, location, and topographical relationship of the sarcoplasmic tubular system.

FIGURE 26 The arrow points to a region where the tubule coming from the Z line (*Z*) joins with a longitudinally oriented tubule (*a*). Note variations in the diameter of the tubules. × 65,500.

FIGURE 27 A typical arrangement of tubules in the region of the Z line (*Z*) (cf. Fig. 30). × 51,500.

FIGURE 28 Very frequently two tubules converge upon a Z line or an M line (cf. Figs. 11, 21, 29). The illustration in Fig. 28 suggests that, at the Z line, the two tubules fuse into one. Note the hint of a possible central membrane (CM). × 54,500.

FIGURE 29 Note the transverse orientation of the tubules from Z line to Z line (*b*, *c*) and the convergence of two tubules at the Z line (*a*). × 57,000.

FIGURE 30 Strand. An interconnecting tubular system at Z. The arrow points to a network of tubules which was rarely encountered. At *H* are one or two vesicular complexes, possibly related to a Golgi apparatus. Note mitochondrion with single central crista (*MS*). × 28,000.

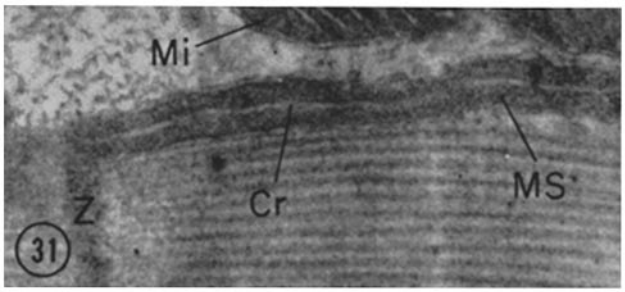

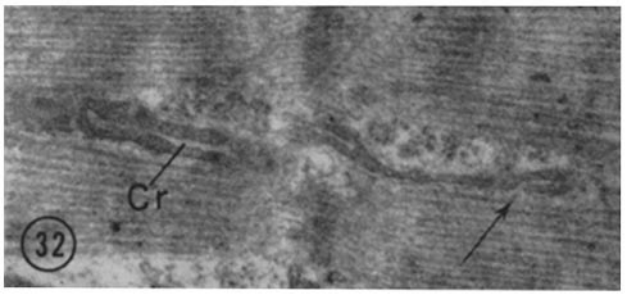

FIGURE 31 Strand. Example of a kind of mitochondrion (*MS*) seen in the strand but not in papillary muscle. Notice its termination at a Z line (*Z*) and its single central crista (*Cr*). *Mi* indicates the kind of mitochondrion seen in both the strand and the papillary muscle. × 74,500.

FIGURE 32 Strand. Similar mitochondria as seen in Fig. 31. The arrow points to a possible origin of the central crista (*Cr*). × 57,000.

of the papillary muscle, are components of the sarcoplasmic reticulum. Based on the structural homology between the couplings of the triads and the peripheral couplings in papillary muscle, on the one hand, and the peripheral couplings of the strand, on the other, the latter are components of the sarcoplasmic reticulum. Thus, the transversely arranged tubules of the strand, too, are parts of the sarcoplasmic reticulum since they are continuous with the couplings (Fig. 21).

The structural homology of the couplings, wherever they occur in the heart muscle, is quite evident, but functional homology, too, has recently been suggested by the localization of ATPase activity in the couplings of the triads, as well as in the peripheral couplings (10, 16, 45, 51, 59). Whereas cytochemical procedures employing lead methods for the demonstration of phosphatases invite cautious interpretation, there is good reason for confidence in the lead methods when they are properly controlled (3, 50). Moreover, the localization of ATPase activity in the regions mentioned above seems particularly reasonable, in view of the fact that Hasselbach recently demonstrated accumulation of calcium within the cisternae of triads (19), an accumulation presumably due to an ATP-driven calcium pump (20).

The experiments of Huxley and Taylor (23) in conjunction with the discovery of the triads (38) and the transverse tubular system (1), as well as the accumulating evidence concerning the functional significance of specific portions of the sarcoplasmic reticulum with respect to the contraction-relaxation cycle (10, 16, 19, 20, 23, 31, 33, 45, 51), all tend to emphasize the significance of the junction between a cisterna of the sarcoplasmic reticulum and the sarcolemma as the anatomical substratum for one step in excitation-contraction coupling. The peculiar configuration of the junction between the terminal cisternae and the sarcolemma has been noted for some time (15, 39), and several authors have described in this region densities displaying a regular periodicity (35, 36, 48) which were interpreted as microtubules by Birks (2). From our studies it appears that these periodic densities are, indeed, small tubules (Fig. 23), or hollow septa, that extend from the terminal cisterna toward the sarcolemma. Occasionally, these tubular processes were met by similar invaginations of the sarcolemma (Fig. 22, long arrow), suggesting, perhaps, that continuity if only transitory, may exist.

With regard to the striae emanating from the sarcolemma of both the strand and the fibers of the papillary muscle, similar structures have been described in other muscles by Ruska (46) who suggested that they represent foci of muscle regeneration. We found these structures very frequently, but not, as Ruska stated, close to nuclei. The characteristic arrangement of the striae with respect to adjacent Z lines suggests a formal sequence of

steps leading to the apposition of new myofibrils of equal length and in register with the already existing sarcomeres (Fig. 35), which would account for an increase in the width of a sarcomere as, for example, in hypertrophy of muscle. Correspondingly, the presence of active striae at the ends of the myofibril would lead to an increase in length (Fig. 37, cf. reference 24).

The morphological features having been discussed on their own merit, it is now appropriate to develop some of the more immediate conclusions of physiological significance to be drawn from the present investigation.

If the membrane complex of the zonula occludens is assumed to be of low electrical resistance compared with the sarcolemma (for discussion, see 9, 44), the distribution of such membrane appositions, as exemplified by those of 185 serial sections of a strand displayed in Fig. 7, represents the pattern of low resistance interconnections between fibers in the strand.

It is clear from Fig. 7 that the strand cannot be treated, electrophysiologically, as a single leaky, capacitive cable. There does not seem to be any recognizable form to the extent and frequency of fiber occlusions. Hence, we cannot suggest a straightforward model of the connections so formed that could allow us to derive, theoretically, a unique relation between the input resistance at any point and the membrane and core resistivities of the fibers forming the network. Nevertheless, approximations can be made that can provide an insight into the effects of such interconnections and indicate a range of probable relationships between the input resistance and the membrane and core resistivities.

In our first approximation (see Fig. 38), we have assumed a symmetry in the distribution of fiber interconnections (from the point of injection of current), in both (longitudinal) directions, parallel to the long axis of the strand. A more general model would be one in which the sites of termination of fibers with other fibers can be distributed over a length of the strand and in which a symmetry of such distributions on either side of a point in the fiber is not assumed. Nevertheless, for simplicity, we have made this latter assumption, and we can then consider the fiber interconnections on one side of the site of injection of current in one fiber of the strand. We have approximated the interconnections between the fibers by saying that, at a distance $x = L$ from the point of injection of current, the fiber is connected by low resistance junctions with n fibers (see Fig. 38). That is to say, at the distance $x = L$, the fiber is terminated by the input resistance of n fibers in parallel, $\frac{z}{n}$, where z is the input resistance of an unterminated fiber of infinite length. The input resistance of a fiber, R_p, terminated by an arbitrary resistance, R, is given by (for discussion of transmission line theory, see 27, 29)

$$R_p = z \cdot \frac{R \cosh L/\lambda + z \sinh L/\lambda}{R \sinh L/\lambda + z \cosh L/\lambda}$$

Since, in the present case, R is equal to $\frac{z}{n}$,

FIGURE 33 Strand. Striae (*St*) emanating at regular intervals from the sarcolemma. Note association of one stria with a tubule of the sarcoplasmic reticulum (*SR*; cf. Fig. 34). × 52,000.

FIGURE 34 Papillary muscle. Striae similar to those seen in the strand (cf. Fig. 33). Note narrow invagination of sarcolemma at arrow, similar to that seen in Fig. 36. × 44,000.

FIGURE 35 Strand. Note striae (*St*) peeling off from the sarcolemma to line up with the adjacent Z line, a process that may lead to lateral sarcomere growth. Note also short myofilaments with an M line (arrow) associated with a stria aligned with the Z line on the right, and a stria that is as yet unaligned with the Z line on the left. × 26,500.

FIGURE 36 Strand. Note narrow invagination of sarcolemma (arrow, cf. Fig. 34) which is in register with the general periodicity of the striae. × 28,500.

FIGURE 37 Strand. The position of the striae (*St*) with respect to the Z line (*Z*) seen in this section illustrates a possible step in the events leading to longitudinal addition of sarcomeres as opposed to lateral addition (cf. Figs. 33–36). × 56,000.

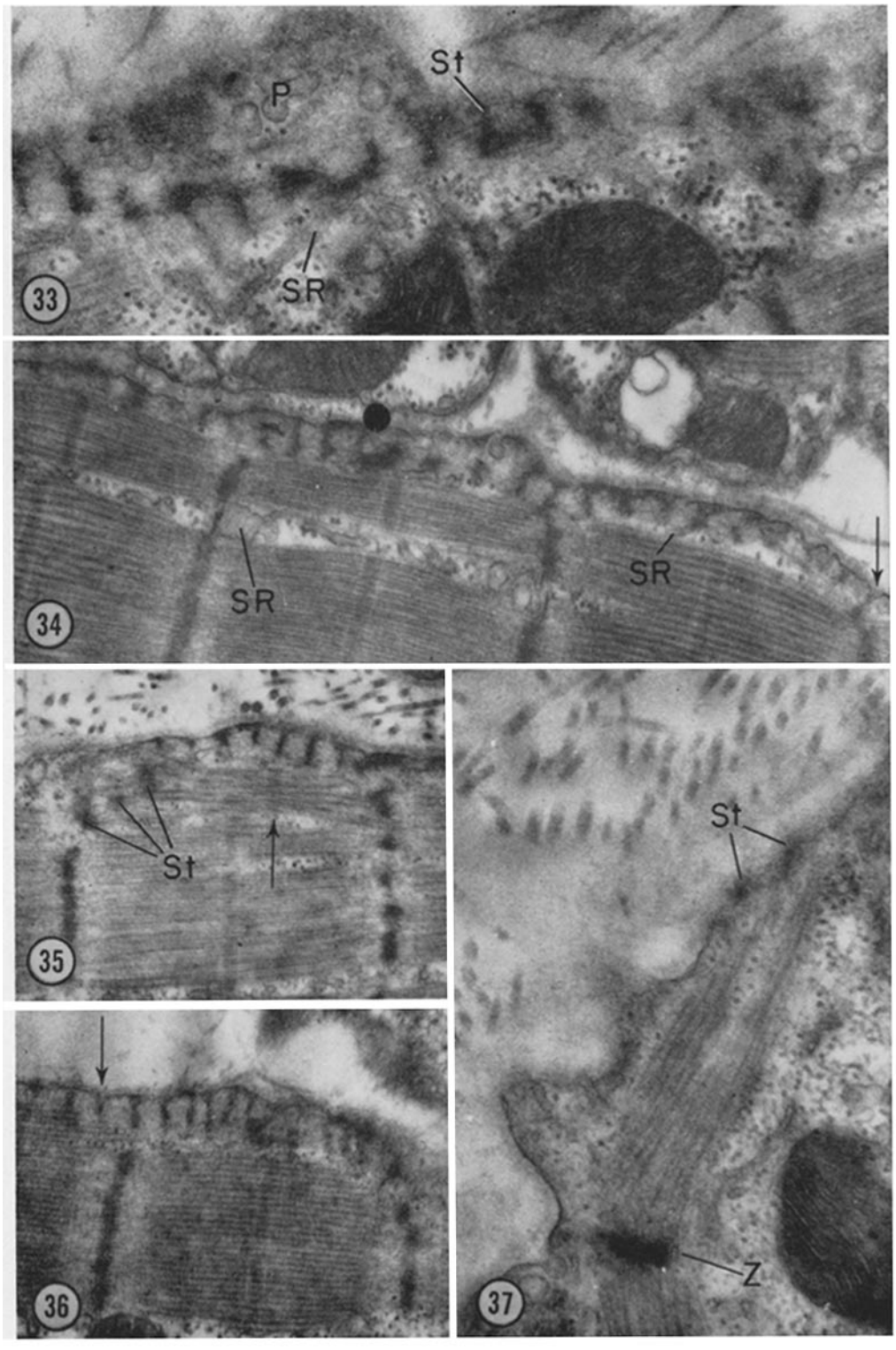
St
P
SR
33
SR
SR
34
St
35
St
Z
37
36

$$R_p = z \cdot \frac{\frac{1}{n}\cosh L/\lambda + \sinh L/\lambda}{\frac{1}{n}\sinh L/\lambda + \cosh L/\lambda}$$

where $\lambda = \sqrt{\frac{r_m}{r_i}}$ and $z = \sqrt{r_m r_i}$; r_m is the membrane resistance times unit length of the fiber, and r_i is the axial resistance per unit length, of a fiber of 10μ in diameter. The relationships between R_p and the membrane resistance, R_m (ohms cm^2), for various values of n and L are shown in Fig. 39. In this figure the values of R_p will be halved, if we consider a symmetrical distribution of a system of cables on both sides of the site of current injection. It is clear from the figure that it is not possible in this system to determine the membrane resistance, knowing r_i and R_p alone. It is not feasible to determine n and L experimentally. Thus, for a given site in a fiber in a strand, the relationship between R_p and R_m is indeterminate, except for large and low values of membrane resistivity relative to 10–1000 ohms cm^2 Under such circumstances, R_p for large values approaches $\frac{z}{n}$, and for low values it approaches z.

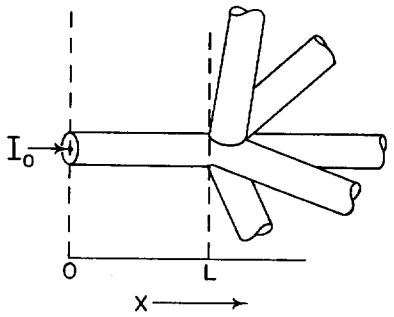

FIGURE 38 A model system of cables, approximating the geometry of interfiber low-resistance connections on one side of the site of injection of current in a fiber in the strand. Current I_0 is injected, at $x = O$, into a single cable which is terminated, at $x = L$, by n cables (in this case, 5).

Assuming a membrane resistance of 1000 ohms cm^2, a core resistivity of 150 ohms cm, and an average fiber diameter of 10 μ, the input resistance presented by a fiber terminated at a distance of 20 μ at either side of the point of injection of the current by five to ten cables is approximately 500K–1M ohms. This value is within the same order of magnitude as that observed experimentally (Johnson, E. A. Unpublished observations).

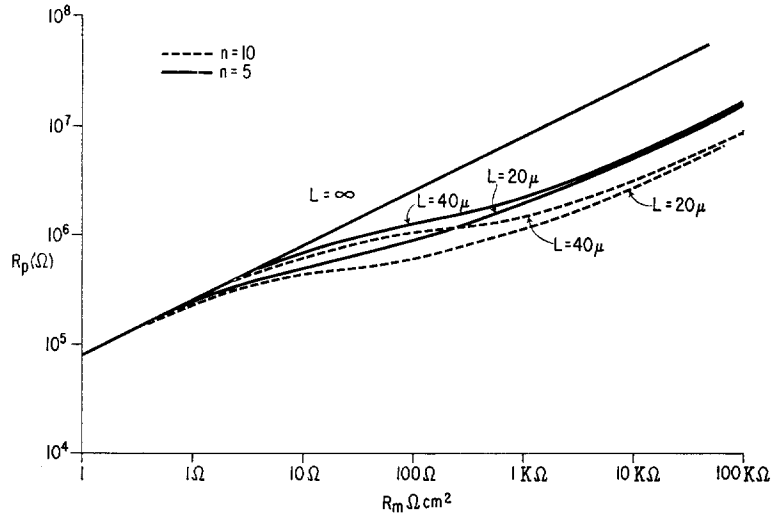

FIGURE 39 Relationship between the input resistance, R_p, as a function of membrane resistance, R_m, for a cable terminated at a distance, L, from one end by n cables. Cable diameter equals 10 μ; volume resistivity of core conductor equals 150 ohms cm. $L = \infty$ corresponds to the case of an unterminated cable, i.e. a single cable of infinite length. For current injected into the center of such a cable and for the case in which there is symmetrical distribution of cables on both sides of the point of current injection (cf. Fig. 38), the values of R_p on the ordinate will be half of the values shown.

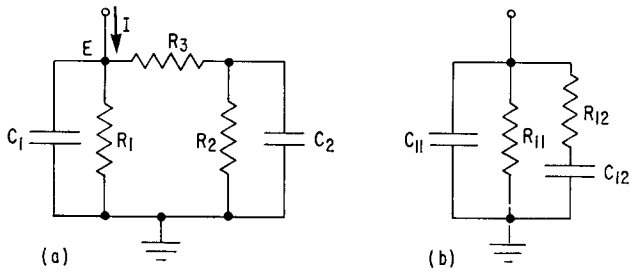

FIGURE 40 (*a*) Lumped equivalent electrical circuit of the system of leaky capacitive cables shown in Fig. 39. (*b*) Circuit electrically equivalent to Fig. 40 (*a*) (has same impedance function) and identical to that used by Fatt and Falk (11) to describe the linear electrical properties of frog skeletal muscle fibers.

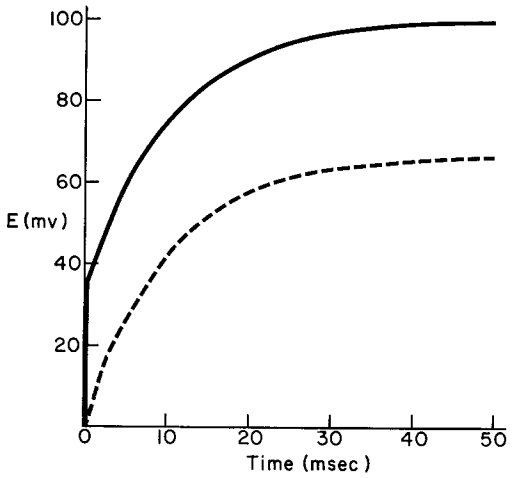

FIGURE 41 Transient response of circuit in Fig. 40 (a) to a step function of current I_0. Dotted line: case (1) in which $R_1 \gg R_2, R_3 = 0$, $R_2 = 787\ K$, $R_2C_2 = 10$ msec. Solid line: case (2) in which $R_1 \gg R_2$, $R_2 = 787K$, $R_3 = 390K$, $R_2C_2 = 10$ msec. $I_0 = 84.96\ nA$ for both cases. These values of R_2 and R_3 were calculated for the situation where $n = 10$, $R_m = 1000\Omega$ cm^2, $R_i = 150\Omega$ cm, and the fiber diameter equals 10 μ, and, in addition, for case (2), $L = 20\ \mu$.

The analysis of the transient response for such a system of cables shown in Fig. 38, i.e. the transient changes in input potential following a step change in input current, is very difficult. Some insight into this transient response can be secured by studying that of a simplified network in which the distributed R and C of the cables are lumped to give the circuit shown in Fig. 40 (*a*). R_1 and C_1 represent the lumped parallel capacitance and resistance of the membrane, and R_3 represents the core resistance, of the short length of cable, $L \ll \lambda$, before its termination by n cables. The input resistance of these n parallel cables is represented by $R_2 = \frac{z}{n}$, and C_2 is chosen such that $R_2 \cdot C_2$ is equal to $R_1 \cdot C_1$, since we assume the properties of the membrane of all cables to be the same. We shall consider a step function of current, I_0, injected at the point indicated in the diagram, and we shall examine the change in potential, E, as a function of time at the point of current injection, $E(t)$. Let us consider the following two cases.

1. L, (or R_3), tends to zero. In this case, $E = E_\infty\ (1 - e^{-t/\tau})$ where τ equals $\frac{R_1 R_2}{R_1 + R_2} \cdot (C_1 + C_2)$. That is to say, E would change exponentially with time, to approach its steady state value $E_\infty = I_0 \cdot \frac{R_1 R_2}{R_1 + R_2}$, as illustrated in Fig. 41 (Case 1).

2. $R_3 \approx R_2$; $R_1 \gg R_2$ or R_3. $E(t)$ is given by the sum of two exponentially varying functions of time, one term reaching its steady state value much more quickly than the other term. $E(t)$ thus shows a sharp inflection that marks the change between the two exponential terms, as illustrated in Fig. 41 (Case 2). Other cases are possible, e.g. $R_2 \ll R_3$ and $R_1 \gg R_2$, but we consider that it would be more appropriate to discuss them elsewhere in relation to a more detailed description of the electrophysiological behavior of the strand.

The two kinds of wave forms given by these two cases have been observed experimentally in the strand. That is to say, for a step function of current injected into a fiber in the strand, $E(t)$ (where E is recorded close to the site of current injection) can be a relatively smooth function of time, as in Fig. 41 (Case 1), or look like Fig. 41 (Case 2). Were the sites of termination of the fibers distributed over a length of the strand rather than at a single point, the transition between the two components of the wave form in Fig. 41 (Case 2) would be less noticeable. The wave form would, in fact, approach that for the distributed circuit form of Fig. 40 (*b*) (11).

Fozzard (14) concluded, from the results of his studies of the passive electrical properties of

Purkinje fibers of the sheep, that part of the membrane capacitance was in series with a resistance. His equivalent network for an element of the fiber membrane is that of Fig. 40 (*b*) and is identical to the two time constant network model put forward by Falk and Fatt (11) to account for their analysis of the linear properties of frog skeletal muscle fibers.

Those authors, in their physical interpretation of such a network, do not discuss the fact that the *RC* network of Fig. 40 (*b*) is equivalent to a number of other *RC* networks (55), e.g. the lumped equivalent network for the strand cable model of Fig. 40 (*a*). Assuming that the fibers of the Purkinje bundle of the sheep are like those of the rabbit strand, then the cable model in Fig. 40 (*a*) provides an alternative explanation for Fozzard's findings. Indeed, in the case of the rabbit strand, a transverse tubular system does not exist, at least of sufficient extent, that would allow an interpretation to be made in terms of a transverse tubular system such as that suggested by Fozzard for Purkinje fibers. Moreover, in one respect, Fozzard's findings are more accurately accounted for by the model system of cables of Fig. 38. He observed that the current required to establish a sudden change in membrane potential at a point in a fiber showed a sharp inflection between a fast and a slow component. Such an inflection would occur in the system of cables of Fig. 38, the equivalent circuit of which approaches closely the lumped circuit of Fig. 40 (*a*). On the other hand, a physical interpretation of the circuit of Fig. 40 (*a*) or (*b*), in terms of a surface membrane and a transverse tubular system of membrane, as proposed by Fatt and Falk (11) and suggested also by Fozzard (14), would require the electrical behavior to approach the distributed form of these circuits. In this case, no sharp inflection would be expected in the current wave form referred to above.

The unpredictable extent and distribution of low resistance connections between fibers in the strand seriously reduces the feasibility of applying, satisfactorily, a voltage-clamp technique utilizing microelectrodes to determine the dependency of the ionic conductances of the fiber membrane upon voltage and time. Even if a small segment of the strand were effectively isolated, electrically, from the rest of the strand, e.g. between two ligatures that constricted the fibers (8), the isolated segment could not be treated, safely, as a single cable-like structure of membrane. Where the equivalent network of the preparation is approximated by the circuit of Fig. 40 (*a*), it is not possible, because of the resistance R_3, to charge simultaneously the capacitors C_1 and C_2, stepwise, to the same potential.

The absence of triads would seem to imply a minimum delay between excitation and contraction. This delay would be the time required for a substance to diffuse from the surface sarcolemma to a certain concentration at the center of the fiber. Calculations show that a time of approximately 12 msec would be required for a substance with a diffusion constant of 10^{-5} cm^2 sec^{-1} to diffuse from a constant concentration immediately outside or in the sarcolemma and reach a concentration, in the center of a cylindrical fiber of 10 μ in diameter, 90% of that immediately outside or in the membrane. Preliminary studies show that the time between the upstroke of an action potential initiated at a point in a fiber in the strand and the movement of sarcomere striations at this point is between 20 and 40 msec. This is not to suggest that this observed delay between excitation and contraction is due to such a diffusion delay, but that a delay does exist which is not in conflict with the time required for such diffusion.

The excellent technical assistance of Mr. Isaiah Taylor is gratefully acknowledged.

The results of this study were presented in part at the meetings of the Federation of American Societies for Experimental Biology, Atlantic City, New Jersey, April 9–14, 1965.

This research was supported by grants from the United States Public Health Service No. HE08620-01, 02, 03, and the Life Insurance Medical Research Fund # G-65-10.

Received for publication 12 May 1966.

REFERENCES

1. ANDERSSON-CEDERGREN, E. 1959. *J. Ultrastruct. Res.* 1 (Suppl): 1.
2. BIRKS, R. I. 1965. *In* Muscle. W. M. Paul, E. E. Daniel, C. M. Kay, G. Monckton, editors. Pergamon Press, Oxford-London-Edinburgh-NewYork-Paris-Frankfurt. 199.
3. BLUM, J. J. 1965. *J. Cell Biol.* **24**:223.
4. BRANDT, P. W., J. P. REUBEN, L. GIRARDIER, and H. GRUNDFEST. 1965. *J. Cell Biol.* **25**: 233.
5. BRIGHTMAN, M. W., and S. L. PALAY. 1963. *J. Cell Biol.* **19**:415.

6. CAESAR, R., G. A. EDWARDS, and H. RUSKA. 1958. Z. *Zellforsch.* **48**:698.
7. DE THÉ., G. 1964. *J. Cell Biol.* **23**:265.
8. DECK, K. A., R. KERN, and W. TRAUTWEIN. 1964. *Pflügers Arch. ges. Physiol.* **280**: 63.
9. DEWEY, M. M., and L. BARR. 1964. *J. Cell Biol.* **23**:553.
10. ESSNER, E., A. B. NOVIKOFF, and N. QUINTANA. 1965. *J. Cell Biol.* **25**:201.
11. FALK, G., and P. FATT. 1964. *Proc. Roy. Soc. (London), Ser. B.* **160**:69.
12. FARQUHAR, M. G., and G. E. PALADE. 1963. *J. Cell Biol.* **17**:375.
13. FARQUHAR, M. G., and G. E. PALADE. 1965. *J. Cell Biol.* **26**:263.
14. FOZZARD, H. A. 1966. *J. Physiol.* **182**:255.
15. FRANZINI-ARMSTRONG, C., and K. B. PORTER. 1964. *J. Cell Biol.* **22**:675.
16. GAUTHIER, G. F., and H. A. PADYKULA. 1965. *J. Cell Biol.* **27**:252.
17. GEORGE, E. P. 1961. *Australian J. Exptl. Biol. Med. Sci.* **39**:294.
18. GRILLO, M. A. 1966. *Pharmacol. Rev.* **18** (1, Pt 1): 387.
19. HASSELBACH, W. 1964. *Federation Proc.* **23**:900.
20. HASSELBACH, W., and M. MAKINOSE. 1963. *Biochem. Z.* **339**:941.
21. HESS, A. 1965. *J. Cell Biol.* **26**:467.
22. HUXLEY, H. E. 1964. *Nature (London).* **202**:1067.
23. HUXLEY, A. F., and R. E. TAYLOR. 1958. *J. Physiol.* **144**:426.
24. ISHIKAWA, H. 1965. *Arch. Histol. Jap.* **25**:275.
25. JOHNSON, E. A., and GAY, W. 1966. *Fed. Proc.* No. 2209. (Abstr.)
26. KAWAMURA, K. 1961. *Jap. Circ. J.* **25**:594.
27. KING, R. W. P. 1965. Transmission Line Theory. Dover Publications, New York.
28. LEDBETTER, M. C., and K. R. PORTER. 1963. *J. Cell Biol.* **19**:239.
29. LE PAGE, W. R., and S. SEELY. 1952. General Network Analysis. McGraw Hill Book Co., New York.
30. MUIR, A. R. 1957. *J. Anat.* **91**:251.
31. MUSCATELLO, U., E. ANDERSSON-CEDERGREN, and G. F. AZZONE. 1962. *Biochim. Biophys. Acta.* **63**:55.
32. NOBLE, D. 1962. *J. Biophys.* **2**:381.
33. PADYKULA, H. A., and E. HERMAN. 1955. *J. Histochem. Cytochem.* **3**:170.
34. PAGE, S. G. 1965. *J. Cell Biol.* **26**:477.
35. PEACHEY, L. D. 1965. *J. Cell Biol.* **25**:209.
36. PEACHEY, L. D., and A. F. HUXLEY. 1962. *J. Cell Biol.* **13**:177.
37. PITELKA, D. R. 1963. Electronmicroscopic Structure of Protozoa. Pergamon Press, The Macmillan Co., New York.
38. PORTER, K. R., and G. E. PALADE. 1957. *J. Biophys. Biochem. Cytol.* **3**:260.
39. REVEL, J. P. 1961. *J. Cell Biol.* **12**:571.
40. REYNOLDS, E. S. 1963. *J. Cell Biol.* **17**:208.
41. RHODIN, J. A. G., P. DEL MISSIER, and L. C. REID. 1961. *Circulation.* **24**:349.
42. RICHARDSON, K. C. 1960. *Stain Technol.* **35**:313.
43. ROBERTSON, J. D. 1959. *Biochem. Soc. Symp. (Cambridge, Eng.)* **16**:3.
44. ROSENBLUTH, J. 1965. *J. Cell Biol.* **26**:579.
45. ROSTGAARD, J., and O. BEHNKE. 1965. *J. Ultrastruct. Res.* **12**:579.
46. RUSKA, H., and G. A. EDWARDS. 1957. *Growth.* **21**:73.
47. SABATINI, D. D., K. BENSCH, and R. J. BARRNETT. 1963. *J. Cell Biol.* **17**:19.
48. SMITH, D. S. 1965. *J. Cell Biol.* **27**:379.
49. SMITH, D. S. 1961. *J. Biophys. Biochem. Cytol.* **10** (4, Suppl.): 123.
50. SOMMER, J. R., and J. J. BLUM. 1965. *J. Cell Biol.* **24**:235.
51. SOMMER, J. R., and M. S. SPACH. 1964. *Am. J. Pathol.* **44**:491.
52. SOMMER, J. R., and J. J. BLUM. 1965. *Exptl. Cell Res.* **39**:504.
53. SPURLOCK, B. O., V. C. KATTINE, and J. A. FREEMAN. 1963. *J. Cell Biol.* **17**:203.
54. TRUEX, R. C. 1961. *In* The Specialized Tissues of the Heart. Elsevier Publishing Co. Amsterdam, London, New York; Princeton. 22.
55. TUTTLE, D. F. 1958. Network Synthesis. John Wiley, New York. 1.
56. VIRAGH, S. Z., and PORTE. A. 1961. *Z. Zellforsch.* **55**:263.
57. WEIDMANN, S. 1952. *J. Physiol.* **118**:348.
58. WIENER, J., D. SPIRO, and W. R. LOEWENSTEIN. 1964. *J. Cell Biol.* **22**:587.
59. ZEBE, E., and H. FALK. 1965. *Histochemie.* **5**:32.